

# Incentivizing Cardiologist-Like Reasoning in MLLMs for Interpretable Echocardiographic Diagnosis

Yi Qin<sup>1</sup>, Lehan Wang<sup>1</sup>, Chenxu Zhao<sup>2</sup>, Alex P.W. Lee<sup>2</sup>, Xiaomeng Li<sup>1\*</sup>

<sup>1</sup>The Hong Kong University of Science and Technology

<sup>2</sup> The Chinese University of Hong Kong

## Abstract

*Echocardiographic diagnosis is vital for cardiac screening yet remains challenging. Existing echocardiography foundation models do not effectively capture the relationships between quantitative measurements and clinical manifestations, whereas medical reasoning multimodal large language models (MLLMs) require costly construction of detailed reasoning paths and remain ineffective at directly incorporating such echocardiographic priors into their reasoning. To address these limitations, we propose a novel approach comprising Cardiac Reasoning Template (CRT) and CardiacMind to enhance MLLM’s echocardiographic reasoning by introducing cardiologist-like mindset. Specifically, CRT provides stepwise canonical diagnostic procedures for complex cardiac diseases to streamline reasoning path construction without the need for costly case-by-case verification. To incentivize reasoning MLLM under CRT, we develop CardiacMind, a new reinforcement learning scheme with three novel rewards: Procedural Quantity Reward (PQtR), Procedural Quality Reward (PQlR), and Echocardiographic Semantic Reward (ESR). PQtR promotes detailed reasoning; PQlR promotes integration of evidence across views and modalities, while ESR grounds stepwise descriptions in visual content. Our methods show a 48% improvement in multiview echocardiographic diagnosis for 15 complex cardiac diseases and a 5% improvement on CardiacNet-PAH over prior methods. The user study on our method’s reasoning outputs shows 93.33% clinician agreement with cardiologist-like reasoning logic. Our code will be available.*

## 1. Introduction

Echocardiography is an essential cardiac imaging modality [40] for assessing a wide range of cardiac diseases [2, 9, 21, 33]. Accurate diagnostic interpretation of echocardiography is challenging and requires comprehensive analysis of heterogeneous inputs [41]. This difficulty is exacerbated in

complex diseases, such as septal defect subtyping [30] or cardiomyopathy [21]. As Fig. 1.c illustrates, clinicians follow a stepwise, logically ordered diagnostic procedure. This process synthesizes multimodal information (e.g., cardiac motion, chamber structure, blood jet velocities, etc.) from multiview echocardiography and quantitative measures, grounded in established cardiac knowledge. Therefore, achieving accurate and reliable echocardiographic diagnosis remains a longstanding challenge for both clinicians and deep learning models.

Recent studies have sought to address this challenge by developing echocardiographic foundation models [1, 6, 10, 38]. However, these models still struggle with complex cardiac diseases (see Tab. 1 row “PanEcho [10]” and “EchoPrime [38]”). For instance, as shown in Fig. 1.a, PanEcho [10] produces contradictory outputs: quantitative measurements and disease classifications suggest opposing diagnoses, e.g., the Left Ventricular Ejection Fraction (LVEF) is below 50%, yet the predicted Left Ventricle (LV) systolic function is labeled as normal. This inconsistency is unreasonable, as most disease classifications are strongly dependent on quantitative measurements [15, 19] (e.g., an LVEF below 50% typically indicates LV systolic dysfunction), which ultimately undermines the model’s reliability.

The main reason for this low reliability is that these models fail to capture the relationships between measurements (e.g., LVEF) and clinical manifestations (e.g., LV systolic dysfunction) when forming diagnostic conclusions. Medical large language models (MLLMs) have recently demonstrated promising reasoning abilities in analyzing clinical questions [11, 13, 22, 26, 34, 35, 39], serving as a potential solution for integrating clinical measurements into the diagnostic decision-making process. However, most of these approaches were primarily developed for general medical image interpretation tasks and lack consideration of domain-specific echocardiographic knowledge, resulting in limited performance when applied directly; see results of “MedVLM-R1 [22]” and “Chiron-o1 [35]” in Tab. 1. A straightforward solution is to incorporate these diagnostic priors by constructing and verifying case-by-case echocardiographic reasoning paths.

\*Corresponding to Xiaomeng Li (eexmli@ust.hk).

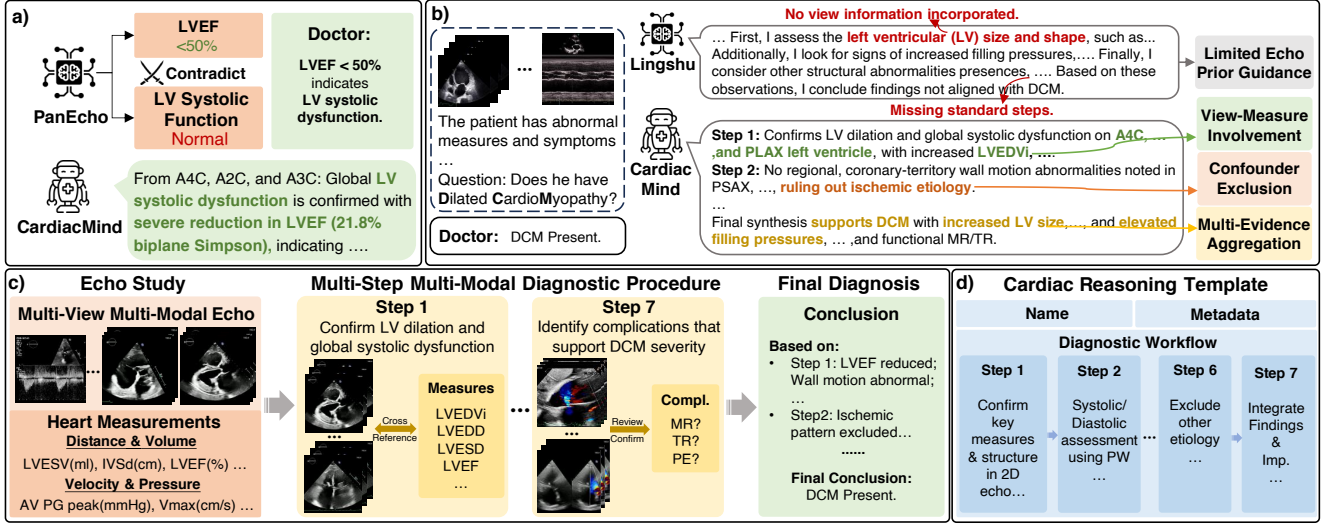


Figure 1. Comparison of CardiacMind with prior methods and overview of the echocardiography diagnosis workflow and the Cardiac Reasoning Template. a) PanEcho [10] predictions versus our model’s reasoning process. b) Reasoning process comparison between the latest medical reasoning method [42] and our model. c) Summary of the dilated cardiomyopathy (DCM) clinical diagnosis workflow [4]. d) Overview of the proposed Cardiac Reasoning Template.

graphic reasoning paths. Nevertheless, this process demands extensive effort from echocardiographers, e.g., more than 450 hours of expert time were required to build chain-of-thought data for only 100 knee scans [27]. Another solution is to directly provide the diagnostic priors as instructions and knowledge on diagnosis for models during inference [45, 46]. However, we found it still achieved limited improvements in echocardiography analysis (row “Qwen2.5-VL-ICL” in Tab. 1).

To address these limitations, we propose a novel approach comprising a Cardiac Reasoning Template (CRT) and a reinforcement learning framework, namely **CardiacMind**, to better enhance MLLMs’ echocardiographic reasoning ability. Our core idea is inspired by the canonical stepwise and deductive diagnostic mindset of cardiologists (Fig. 1.c). To streamline the construction of reasoning paths, the CRT provides stepwise echocardiographic diagnostic procedures that emulate cardiologists’ diagnostic logic, incorporating knowledge distilled from authoritative sources to guide the model’s reasoning during both training and inference. As Fig. 1.d shows, CRT provides accurate and concise guidance that directs the model to perform detailed analysis, addressing the previous costly data construction demand while effectively introducing echocardiographic reasoning prior.

To incentivize MLLM under CRT, we introduce **CardiacMind**, a reinforcement learning framework with three novel rewards: the Procedural Quantity Reward (PQtR), the Procedural Quality Reward (PQIR), the Echocardiography Semantic Reward (ESR). PQtR and PQIR supervise the model by evaluating the extensiveness and content relevance of reasoning steps relative to the CRT, thereby promoting the logical integration of diagnostic evidence across multi-

modal and multiview echocardiographic inputs. ESR further strengthens the alignment between the descriptive content produced under PQIR guidance and the echocardiographic video content, enabling faithful interpretation of echocardiography. During inference, we further introduce Template-guided Reasoning Rectification (TRR) within CardiacMind, which leverages the CRF to detect and correct deviations from procedural steps, thereby refining the model’s final diagnostic conclusions. To summarize, our key contributions are listed as follows:

- We introduce Cardiac Reasoning Template (CRT), the first high-level concise echocardiographic diagnostic reasoning path for 15 types of complex cardiac diseases, acting as the anchor for the echocardiographic reasoning model.
- We propose CardiacMind, a new rule-based reinforcement learning method that leverages CRT to incentivize MLLM’s rigid cardiologist-like diagnostic reasoning through three novel rewards.
- Our results demonstrate a 48% accuracy improvement in multiview, multimodal echocardiographic diagnosis for 15 complex cardiac diseases and a 5% accuracy improvement on single-view CardiacNet-PAH benchmarks over prior methods. The user study on our method’s reasoning outputs shows 93.33% clinician agreement with cardiologist-like reasoning logic.

## 2. Related Works

### 2.1. Medical Reasoning Multimodal Large Language Models

Recent medical reasoning multimodal large language models [11, 13, 22, 34, 35, 39, 42] demonstrate improved per-

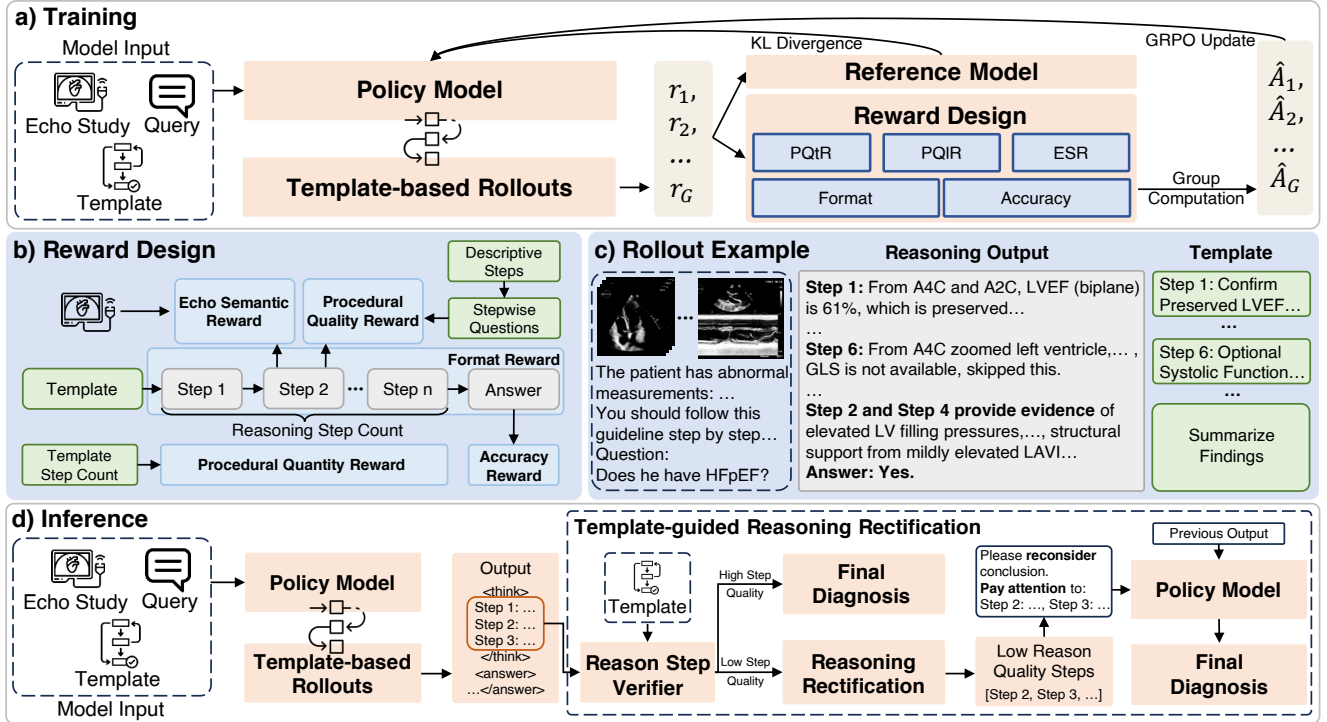


Figure 2. Overview of CardiacMind. a) Training. CardiacMind uses Group Relative Policy Optimization with three novel rewards and two basic rewards. b) Reward design. We introduce three new rewards that encourage extensive reasoning aligned with standard diagnostic procedures. Elements in Green indicate contents from the CRT template. c) Example of the reasoning process. d) Inference. CardiacMind supports scalable inference through template retrieval and Template-guided Reasoning Rectification (TRR). TRR monitors and corrects steps that deviate the prescribed procedure and it refines the final conclusion.

formance on medical diagnosis by analyzing questions step by step. MedVLM-R1 [22], Med-R1 [13], and GMAI-VL-R1 [34] use rule-based reward functions with Group Relative Policy Optimization (GRPO) to extend the reasoning process. MedE<sup>2</sup> [11] constructs a reasoning database and applies Direct Preference Optimization (DPO) to further enhance reasoning. Chiron-o1 [35] introduces a new reasoning path search scheme to build rigorous and effective medical reasoning data. MedRwR [39] further improves reasoning by actively retrieving referential content during the reasoning process. Unlike prior work that either requires costly, case-by-case reasoning-path constructions to inject diagnostic priors [11, 35, 39] or provides only limited supervision of the diagnostic reasoning process during training [13, 22, 34], our CRT streamlines reasoning-path construction by distilling canonical stepwise diagnostic procedures into high-level, accurate guidance supporting the model’s detailed analysis. This approach substantially reduces the cost of reasoning-path construction while effectively introducing authoritative, stepwise reasoning guidance for the model.

## 2.2. Reasoning Models with Trajectory Guidance

Recent methods guide model reasoning with external knowledge using templates [45, 46], process reward models [47],

50], or stepwise supervision [16, 27, 48]. ReasonFlux retrieves hierarchical templates at inference to provide step by step guidance for math problems [46]. Med-PRM [47] uses retrieval augmented generation to verify each step against medical knowledge bases. R1-VL introduces stepwise rewards to promote accuracy and logical coherence [48]. However, directly providing such guidance only at inference for multimodal echocardiographic reasoning yields limited improvements, and constructing case-by-case guidance remains costly. In contrast, CardiacMind introduces three novel rewards within a reinforcement learning framework that encourage the model to perform detailed stepwise reasoning under the high-level instructions from CRT, without requiring case-by-case ground-truth guidance, while strengthening its association with echocardiographic content. These rewards incentivize the MLLM’s echocardiographic reasoning ability, thereby enhancing its performance under complex diseases.

## 3. Methodology

### 3.1. Cardiac Reasoning Template

We first construct **Cardiac Reasoning Template (CRT)** as the anchor reasoning trajectory for CardiacMind. As shown

in Fig. 1.d, each CRT template summarizes a stepwise echocardiographic diagnosis procedure distilled from textbooks and guidelines. Each step provides a high-level reasoning direction that guides the model to analyze and integrate echocardiographic evidence for deductive diagnosis, mirroring the workflow of cardiologists. The steps contain only high-level summaries of diagnostic procedures and exclude any patient-specific conclusions to prevent data leakage.

To construct CRT, we select 15 complex cardiac diseases to ensure the coverage of clinically relevant conditions. We define complex cardiac diseases as conditions that require establishing a diagnosis using evidence from more than three echocardiographic views and measurements. Next, we use an automatic pipeline [23] to retrieve and process transthoracic echocardiography (TTE) guidelines and relevant textbooks and to organize them into a structured database. We then prompt GPT-5 to convert long, descriptive paragraphs into concise, stepwise diagnostic procedures for each disease. A board-certified cardiologist validated the CRT. We provide further details and complete examples in Supplementary Sec. B.

Figure 1.d illustrates the CRT template structure. Each template comprises three components: Template Name, Metadata, and Diagnostic Workflow. **Template Name** is the name of the template, denoted as  $T_{name}$ . **Metadata**  $T_{meta}$  contains keywords and a concise summary to facilitate retrieval. Specifically,  $T_{meta}$  includes four fields: “Knowledge Tag”, which lists key diagnostic concepts in the procedure; “Description”, which provides a brief summary of the diagnostic process; “Application Scenario”, which lists disease-specific abnormalities to consider; and “Views and Measurements Required”, which lists the echocardiographic views and measurements needed for analysis.  $T_{name}$  and  $T_{meta}$  serve as the retrieval key for CRT. A template is defined as  $T = \{T_{name}, T_{meta}, T_{reason}\}$ . The complete CRT is the collection of all templates, denoted as  $\mathcal{T} = \{T_1, T_2, \dots, T_n\}$ , where  $n$  is the total number of reasoning templates. We constructed  $n = 42$  templates in total.

During training, we retrieve the disease-specific template from CRT using  $T_{name}$  and  $T_{meta}$ . We include the retrieved template in the model input. We design three rewards that enforce adherence to the diagnostic procedure and promote effective use of echocardiographic evidence. During inference, we use the disease query to retrieve the template with the same strategy and include it in the model input. CRT also enables inference scaling to improve reasoning reliability and accuracy, as detailed in Sec. 3.3.

### 3.2. Echocardiographic Multi-Modal Reasoning with Template Guidance

#### 3.2.1. Problem Formulation

We formulate the task as a visual question answering problem. The input is multimodal,  $x = \{[v_k]_{k=1}^K, t\}$ . It com-

prises  $K$  echocardiographic inputs  $[v_k]_{k=1}^K$  with view labels assigned by a strong view classification model [32]. It also includes a text component  $t$  that specifies the disease query and lists echocardiographic and measurement abnormalities. This input setup mirrors clinical practice. We model the MLLM as a policy  $\pi_\theta(\cdot|x, T)$  that performs autoregressive generation given  $x$  and the retrieved reasoning template  $T \in \mathcal{T}$  from CRT. The policy first outputs a sequence of  $i$  reasoning steps  $R = \{h_1, h_2, \dots, h_i\}$  under template guidance. It then outputs the final disease diagnosis  $y$ .

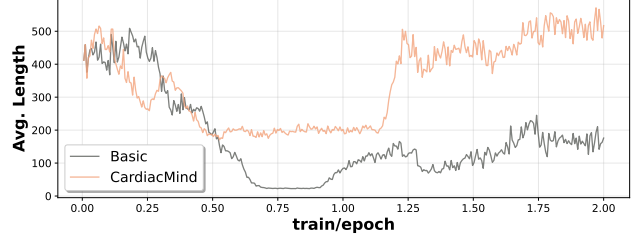


Figure 3. Average response length during training. “Basic” uses only accuracy and format rewards and yields short reasoning without detail on complex echocardiography inputs. CardiacMind first preserves a stepwise reasoning structure in the first training stage (epoch 0-1). It is then incentivized to produce detailed stepwise diagnostic reasoning in the second training stage (epoch 1-2).

#### 3.2.2. Reward Design

We propose three rewards that leverage the curated CRT. These rewards guide the model to produce detailed and factually grounded analyses of the echocardiographic inputs with adherence to the template, as shown in Fig. 2.b.

**Procedural Quantity Reward.** We propose the Procedural Quantity Reward (PQtR)  $\sigma_{PQtR}$  to encourage extensive stepwise reasoning. As shown in Fig. 3, complex echocardiography inputs often prevent the model from establishing an accurate and long reasoning path. In response, the model reduces its reasoning process to minimize apparent errors. Such reduction weakens logical support and can still lead to incorrect conclusions. It also undermines subsequent reward modeling for stepwise diagnostic content. To counter this effect, PQtR counts the number of generated reasoning steps and compares it with the reference step count in the template. The reward encourages the model to produce explicit reasoning steps with a similar count to the reference. We formally define PQtR in Eq. (1).

$$\sigma_{PQtR} = \begin{cases} \min(1.0, \frac{|R|}{|T|}), & \text{if } |R| \leq |T| + \epsilon \\ 0, & \text{otherwise.} \end{cases} \quad (1)$$

In Eq. (1),  $|R|$  and  $|T|$  denote the number of steps in the model’s reasoning and in the reference template, respectively. The verbosity tolerance threshold  $\epsilon$  regularizes the generation of reasoning steps and keeps the step count within a reasonable range. This allows the model to analyze and then summarize information when needed. We set  $\epsilon = 5$  in all experiments.

**Procedural Quality Reward.** While PQtR encourages extensive stepwise reasoning, the model must also adhere to standard diagnostic procedures and aggregate heterogeneous evidence in each step. We therefore propose the Procedural Quality Reward (PQIR)  $\sigma_{PQIR}$ . It measures the stepwise relevance of the generated reasoning with respect to the retrieved reasoning templates.

Specifically, for each diagnostic step  $a_m$  in the retrieved templates  $T_{reason} \in \mathcal{T}$ , we convert its description into a list of  $P$  echocardiography centered questions  $a_m \rightarrow [q_m^p]_{p=1}^P, P \leq 5$  that target echocardiographic views and cardiac measurements (details in Supplementary Sec. C.1). We discard questions that require views unavailable for the specific patient by using  $T_{meta}$ . This avoids requesting nonexistent observations. Finally, for each corresponding reasoning step  $h$  produced by the model  $\pi_\theta$ , we apply an external verifier  $g(h, q) \rightarrow [0, 1]$  to score  $h$  for content relevance, logical coherence, and conclusiveness with respect to  $q$ . Equation (2) gives the formal definition of PQIR.

$$\sigma_{PQIR} = \begin{cases} \frac{\sum_{i=1}^{|T|} g(h_i, [q_i^p]_{p=1}^P)}{|T|}, & \text{if } |T| \leq |R| \leq |T| + \epsilon \\ 0, & \text{otherwise.} \end{cases} \quad (2)$$

Here,  $h_i \in R$  and  $[q_i^p]_{p=1}^P \in Q$ .  $R$  is the set of generated reasoning steps.  $Q$  is the set of question lists. The verifier  $g$  produces a single score for one question set  $[q_i^p]_{p=1}^P$ . We compute the reward only when the total number of reasoning steps at least reaches that of the template, ensuring that the reasoning content is evaluated at the correct steps.  $\epsilon$  is the verbosity tolerance threshold, identical to that used in PQtR. We implement the verifier  $g$  using the LLM-as-Judge strategy [17] with Qwen3-8B [43]. See Supplementary Sec. C.2 for details.

**Echocardiographic Semantic Reward.** To ensure faithful analysis, the echocardiographic descriptive content in the stepwise reasoning promoted by PQtR and PQIR must be aligned with the visual input. We therefore propose the Echocardiographic Semantic Reward (ESR)  $\sigma_{ESR}$  to enforce visual grounding. ESR encourages agreement between each video and its corresponding description in the reasoning steps by maximizing their embedding cosine similarity. At each generated reasoning step, we identify sentences  $s$  that contain echocardiographic view names that capture the descriptive content. For each such sentence, we use the view name to retrieve the corresponding video  $v$  and construct the set of paired video and sentence data  $V = \{(v_i, s_i)\}$ . We then use a CLIP-based echocardiography visual language model [38], denoted  $f(v, s)$ , as the verifier. Given a pair,  $f(v, s)$  computes the text video embedding cosine similarity and normalizes it to the range  $[0, 1]$ . The formal definition of ESR is given in Eqn. 3.

$$\sigma_{ESR} = \begin{cases} \frac{\sum_{i=1}^{|V|} f(v_i, s_i)}{|V|}, & \text{if } |T| \leq |R| \leq |T| + \epsilon \\ 0, & \text{otherwise.} \end{cases} \quad (3)$$

Here,  $|V|$  denotes the total number of pairs. The reward calculation threshold is identical to that used in PQIR. Note that  $f(v, s)$  verifies video with single descriptive sentence instead of composite final diagnostic conclusion, thereby decreasing the difficulty of accurate text-video similarity estimation.

**Format and Accuracy Reward.** We apply basic format and accuracy rewards to enforce the output structure and the correctness of the final conclusion. For the format reward  $\sigma_{format}$ , the model must wrap the reasoning process in `<think>/</think>` and the final conclusion in `<answer>/</answer>`. The format reward is 1 if the model complies with this specification and 0 otherwise. For the accuracy reward  $\sigma_{acc}$ , we extract the answer from `<answer>/</answer>` and compare it with the ground truth. The accuracy reward is 1 if the extracted answer matches the ground truth and 0 otherwise.

**Hallucination Reduction Gating.** The correctness of the diagnostic conclusion is paramount. To discourage responses that appear superficially reasonable but yield wrong conclusions, we introduce a hallucination reduction gate. It sets our proposed reward to zero when the final answer is incorrect. The gating mechanism is formulated as  $\delta(\cdot) = \mathbf{1}\{\sigma_{acc} = 1\}$ .

**Overall Reward.** We combine all rewards with reweighting to balance the reward contribution using linear weights  $\lambda$ . The final reward calculation is shown as Eq. (4).

$$\sigma = \lambda_{format}\sigma_{format} + \lambda_{acc}\sigma_{acc} + \delta(\lambda_{PQIR}\sigma_{PQIR} + \lambda_{PQtR}\sigma_{PQtR} + \lambda_{ESR}\sigma_{ESR}) \quad (4)$$

### 3.2.3. Training Procedure

**Reinforcement Learning Algorithm.** We adopt Group Relative Policy Optimization (GRPO) [29] as the reinforcement learning strategy, employing the proposed reward functions to enhance the model’s exploration capability in complex echocardiography analysis, as illustrated in Fig. 2.a. The complete GRPO objective used for optimization is calculated as shown in Supplementary Sec. D.2.

**Two Stage Training Strategy.** To encourage extensive procedure aligned reasoning while preserving diagnostic performance, we adopt a two stage training strategy [26, 39]. We base all training on the Qwen 2.5-VL-7B model [3]. In stage one, the model is trained with the format, accuracy, and procedural quantity rewards. This stage consolidates core echocardiography recognition across multiple views and modalities and preserves a stepwise reasoning structure. We set  $\lambda_{format} = 1$ ,  $\lambda_{acc} = 1$ ,  $\lambda_{PQtR} = 1$  in this stage. In stage two, we apply the complete reward model during

training to align the model’s reasoning trajectory with anchor diagnostic procedures. We set  $\lambda_{format} = 1$ ,  $\lambda_{acc} = 1.5$ ,  $\lambda_{PQlR} = 0.8$ ,  $\lambda_{PQtR} = 0.5$ , and  $\lambda_{ESR} = 0.5$  in this stage.

### 3.3. Template-guided Reasoning Rectification

Building on CRT, we propose Template guided Reasoning Rectification (TRR) for scalable inference in CardiacMind. As Fig. 2.d shows, during inference we first retrieve a reasoning template from CRT using the disease query. The trained model then follows this template to generate stepwise reasoning. Figure 2.c shows an example of the reasoning process with the complete echocardiography study and the retrieved template as inputs.

After the model completes reasoning, we reuse the verifier and scoring rule from the Procedural Quality Reward (Sec. 3.2.2) as the reasoning step verifier. This verifier scores each step against the retrieved template and outputs a step quality score. If the average step quality exceeds a preset threshold, we accept the conclusion as compliant with standard procedures and return it as the final output. If the average step quality is below the threshold, we prompt the model again using the previous reasoning path and highlight steps with low template adherence. The prompt instructs the model to reconsider and attend to these flagged elements. We then return the revised conclusion as the final output. We empirically set the threshold to 0.4 in our experiments.

## 4. Experiments

### 4.1. Experiment Settings

**Development Data and EchoComplex.** To the best of our knowledge, no public echocardiography dataset spans multiple views and modalities for diagnosing complex cardiac diseases<sup>1</sup>. We therefore curated a training dataset and a test dataset from our collaborating hospital. The training dataset contains 1,486 patients covering 15 disease categories. Each patient has a complete echocardiographic study with annotated view labels, quantitative measurements, and a diagnostic report confirmed by cardiologists. Disease labels were derived from these reports. In total, we constructed 2,550 labeled training instances with both positive and negative examples. To benchmark models’ ability for multiview, multimodal echocardiographic reasoning at complex diseases, we curate a test set, EchoComplex, comprising 623 patients across the same 15 categories. It matches the data composition of the training dataset. From it, we created 846 diagnostic questions about cardiac diseases for testing. Institutional Review Board approved this disidentified study. Further details are provided in Supplementary Sec. A.

**Public Benchmarks.** We further evaluate generalization to single view echocardiographic diagnosis using two public

benchmarks, CardiacNet-ASD and CardiacNet-PAH [44]. They provide apical four chamber (A4C) echocardiography videos for diagnosing pulmonary hypertension (PAH) and atrial septal defect (ASD).

**Baseline Methods.** We conduct extensive comparisons across four categories of baseline models. (1) Echocardiography foundation models, which are discriminative models pretrained on large echocardiography datasets. (2) General multimodal large language models (MLLMs) designed for general purpose visual question answering. (3) Generalist medical MLLMs trained on diverse multimodal medical data. (4) Reasoning oriented medical MLLMs optimized for explicit reasoning over medical images. We provide implementation details for baselines at Supplementary Sec. E.1.

### 4.2. Main Results

As shown in Tab. 1, our model attains the highest accuracy and F1 score on the multiview EchoComplex dataset and the highest F1 score on the single view CardiacNet benchmarks. Compared with echocardiography foundation models, our method yields higher accuracy on EchoComplex. CardiacMind also surpasses both state-of-the-art medical MLLMs and their reasoning variants on EchoComplex, improving accuracy by 48% compared with medical MLLMs (0.56 vs. 0.83) and by 6% compared with trained reasoning variants. Automatic reasoning quality assessment [24, 39] on the reasoning paths for EchoComplex further indicates that CardiacMind achieves the highest reasoning quality, with a 19% improvement over all baselines. Details of the assessment are provided in Supplementary Sec. E.2. Notably, even without additional training, directly providing the retrieved template as in-context knowledge at inference increases the base model’s accuracy from 0.49 to 0.57 and its reasoning quality from 3.09 to 4.02, indicating the effectiveness of CRT with canonical stepwise guidance and knowledge. These results highlight that CardiacMind can leverage informative templates from CRT for multi-evidence integrated reasoning similar to that of a cardiologist, which is a key factor for clinical trustworthiness and accuracy. At the same time, medical reasoning MLLMs show reduced reasoning quality on echocardiography analysis, suggesting that multiview multimodal echocardiographic reasoning remains challenging.

### 4.3. User Study on Our Results

We further invited a cardiologist to conduct a preference study. We randomly sampled CardiacMind and Ling-Shu [42]’s reasoning for 30 patients. Blinded to model identity, the cardiologist compared paired outputs and selected the superior reasoning path based on three predefined criteria. Details of the user study are provided in Supplementary Sec. E.3. The results in Fig. 4 show that 93.33% of CardiacMind’s reasoning trajectories were judged as “more aligned with Cardiologist Logic”. 73.33% were preferred for

<sup>1</sup>MIMIC-IV-Echo [7] has regional ban and incomplete echocardiography study record, therefore unavailable for this study.

Table 1. Performance on echocardiographic diagnosis benchmarks. Name with “\*” indicates that the model was tuned on the training set. Other models are evaluated directly using the official checkpoints. “-ICL” denotes providing the model with retrieved CRT as input at inference only. “-SFT” denotes supervised finetuning without CRT. “-GRPO” denotes GRPO tuning with accuracy and format rewards [8] without CRT. “RQ” denotes the Reasoning Quality score. We use GPT-5, following the common evaluation protocol [24, 39], to compute scores in the range [0, 5]. “-” denotes no reasoning process in the inference thus unavailable. “Ours” denotes results with both CRT and CardiacMind. Best results are in **bold**. Second bests are in underline. For all metrics, higher is better.

Method	EchoComplex			CardiacNet-ASD		CardiacNet-PAH	
	Accuracy	F1	RQ	Accuracy	F1	Accuracy	F1
Echocardiography Foundation Model							
EchoPrime [38]	0.58	0.66	-	0.43	<u>0.57</u>	0.46	0.42
PanEcho* [10]	0.52	0.10	-	<u>0.56</u>	0.09	0.31	0.07
General MLLM							
Qwen2.5-VL [3]	0.49	0.15	3.09	0.53	0.44	0.31	0.03
Qwen2.5-VL-ICL [3]	0.57	0.46	4.02	0.53	0.45	0.31	0.05
Qwen2.5-VL-SFT* [3]	0.76	0.69	-	0.42	<b>0.59</b>	0.3	0.01
Qwen2.5-VL-GRPO* [3]	0.80	0.77	3.69	0.55	0.27	0.31	0.04
R1-VL* [48]	0.72	0.68	3.01	<b>0.57</b>	0.20	0.31	0.04
Generalist Medical MLLM							
Lingshu [42]	0.56	0.51	3.11	0.45	0.40	0.65	0.77
Lingshu-GRPO* [42]	0.78	0.79	3.07	0.42	<u>0.57</u>	0.66	0.78
MedGemma [28]	0.53	0.46	3.20	0.54	<u>0.57</u>	0.37	0.31
HuatuoGPT-Vision [5]	0.54	0.46	2.17	0.53	<u>0.31</u>	0.40	0.32
Reasoning Medical MLLM							
MedVLM-R1 [22]	0.47	0.43	1.48	0.44	0.41	0.36	0.42
Chiron-01 [35]	0.53	0.44	2.76	0.40	0.34	0.47	0.58
Med-RwR [39]	0.49	0.48	3.00	0.52	0.56	0.47	0.50
<b>Ours</b>	0.83	0.81	4.40	0.48	<b>0.59</b>	<u>0.67</u>	<b>0.79</b>
<b>Ours+TRR</b>	<b>0.84</b>	<b>0.82</b>	<b>4.48</b>	0.49	<b>0.59</b>	<b>0.68</b>	<u>0.78</u>

being more “Clear and Deductive”. 80% were preferred for stronger “View and Measurement Involvement”. These findings indicate that CardiacMind aligns more closely with the clinical diagnostic workflow and is preferred by clinicians.

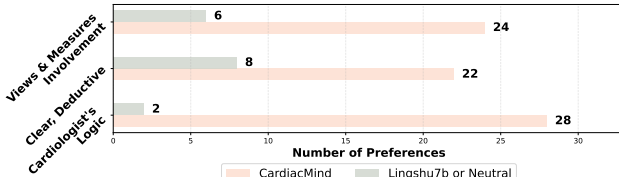


Figure 4. Cardiologist preference result on reasoning quality between our method and LingShu [42]. We assess reasoning quality using three criteria. “Cardiologist’s Logic”: alignment between the reasoning path and cardiologist diagnostic logic. “Clear and Deductive”: clarity and deductive structure of the reasoning process. “View & Measurement Involvement”: explicit use of views and measurements in the reasoning process. A higher preference number indicates that cardiologists judged the reasoning to be of higher quality.

#### 4.4. Ablative Study

##### 4.4.1. CRT and Reward Analysis

We first ablate the proposed reward functions to evaluate their effects on reasoning trajectories and accuracy. The results are shown in Tab. 2. When only accuracy and format rewards are applied, the model maintains decent accuracy on EchoComplex (81%). However, it produces short reasoning trajectories with limited diagnostic insight with reasoning quality score dropping to 3.78. When PQtR and PQIR are applied, both reasoning quality and diagnosis F1 score increase (F1: 0.79 to 0.81, reasoning quality: 3.78 to 4.26). This indicates that PQtR and PQIR guide the model to reason logically and to adhere to standard diagnostic procedures. The best reasoning quality and accuracy are obtained when all three rewards are applied, further demonstrating the effectiveness of the echocardiography semantic reward. Altogether, the three rewards in CardiacMind encourage the model to use this prior knowledge to address critical visual centric challenges and to improve disease diagnosis. Moreover, models trained with basic rewards without CRT yield worse rea-

Table 2. Ablation study of reward functions. All configurations that with CRT include accuracy and format rewards with the retrieved template. Ablations with CRT are performed starting from the checkpoint trained in the first stage. Configuration without CRT use accuracy and format rewards to train two epochs. “RQ” denotes the Reasoning Quality score consistent with Tab. 1. Best results are in **bold**.

Rewards				EchoComplex			CardiacNet-ASD		CardiacNet-PAH	
CRT	PQtR	PQIR	ESR	Accuracy	F1	RQ	Accuracy	F1	Accuracy	F1
✗	✗	✗	✗	0.81	0.78	3.48	<b>0.55</b>	0.27	0.31	0.03
✓	✗	✗	✗	0.81	0.79	3.78	<b>0.55</b>	0.29	0.31	0.05
✓	✓	✗	✗	0.82	0.8	4.06	0.46	0.56	0.33	0.21
✓	✓	✓	✗	0.81	0.81	4.26	0.46	0.56	0.66	0.75
✓	✓	✓	✓	<b>0.83</b>	<b>0.81</b>	<b>4.40</b>	0.48	<b>0.59</b>	<b>0.67</b>	<b>0.79</b>

soning quality, showing the importance of the canonical stepwise knowledge introduced by CRT.

Table 3. Ablation for Procedural Quality Reward on EchoComplex. RQ denotes the Reasoning Quality score, consistent with Tab. 1. “Similarity-Based” maximizes the embedding similarity between the first sentence of each reference step and each step in the model’s reasoning. For “Paragraph Verify”, we feed each step’s descriptive content to the LLM judge rather than converting it into actionable questions.

Design	Accuracy	F1	RQ
Similarity-Based	0.82	0.81	4.31
Paragraph Verify	0.81	0.80	4.23
CardiacMind	<b>0.83</b>	<b>0.81</b>	<b>4.40</b>

#### 4.4.2. Procedural Quality Reward Analysis

The Procedural Quality Reward (PQIR) is the core reward that incentivizes the model to reason following canonical steps and to aggregate heterogeneous information. We therefore evaluate and validate key design choices in PQIR. We consider several alternatives. The first directly maximizes embedding similarity between the first sentence of the reference template’s step and each model step. The similarity is computed based on Qwen3-Embedding-0.6B [49] embeddings. The second feeds the original descriptive sentences to the verifier instead of using actionable questions. Table 3 summarizes the comparison, and Supplementary Sec. G.3 provides representative reasoning outputs for these choices. All alternatives yield comparable diagnosis performance on EchoComplex. This shows that PQIR is a robust way to leverage the high-level content in CRT and to encourage reasoning with multisource information integration. However, using actionable questions with the LLM as Judge scheme yields the best reasoning quality, with a 4% increase. This supports CardiacMind’s design choice of verifying content through direct questions. This strategy simplifies the evaluation of logic-intensive content while still leveraging the high-level semantics provided by the template.

#### 4.4.3. Training Procedure Analysis

We further assessed the necessity of two training components: Hallucination Reduction Gating (HG) and the Ver-

bose Tolerance Threshold (VT). Table 4 shows that removing HG reduces accuracy to 0.79. This suggests that when the model arrives at an incorrect conclusion, the three additional rewards risk diluting the accuracy signal, which HG is designed to prevent. Training without VT causes a slight performance drop. This likely occurs because the model outputs more reasoning steps to pursue a higher PQIR score but fails to effectively aggregate information from verbose outputs. These results validate the necessity of both components.

Table 4. Ablation study of CardiacMind training procedures on EchoComplex. VT denotes the Verbose Tolerance Threshold, and HG denotes Hallucination Reduction Gating.

VT	HG	Accuracy	F1
✓	✗	0.79	0.77
✗	✓	0.81	0.79
✓	✓	<b>0.83</b>	<b>0.81</b>

#### 4.4.4. Template-guided Reasoning Rectification Analysis

We also analyzed the performance gains attributable to Template guided Reasoning Rectification. As shown in Tab. 1, both accuracy and F1 score increase after rectifying the reasoning trajectories for cases with initially low reasoning quality scores. Comparative case studies of the rectification process are provided in Supplementary Sec. G. With the reconsideration prompt, the model explicitly identifies and assesses critical steps that the previous round of reasoning may have neglected. It then revises the final conclusion, which leads to better results.

## 5. Conclusion

In this paper, we present the Cardiac Reasoning Template (CRT) and CardiacMind, a novel approach that systematically embeds cardiologist-like mindset into medical reasoning MLLMs. We curate a library of concise stepwise echocardiographic diagnostic procedures for 15 complex cardiac diseases from authoritative sources. We design a two stage rule based reinforcement framework with three new rewards that promote comprehensive analysis of echocardiography studies and faithful adherence to CRT. We also use CRT to scale inference by assessing and correcting the

reasoning process. Experiments on 15 echocardiographic diagnostic tasks, external validation, and clinical ratings demonstrate the effectiveness of our method.

## References

- [1] Abdoul Aziz Amadou, Yue Zhang, Sebastien Piat, Paul Klein, Ingo Schmuecking, Tiziano Passerini, and Puneet Sharma. Echoapex: A general-purpose vision foundation model for echocardiography. *arXiv preprint arXiv:2410.11092*, 2024. 1
- [2] Elena Arbelo, Alexandros Protonotarios, Juan R Gimeno, Eloisa Arbustini, Roberto Barriales-Villa, Cristina Bassi, Connie R Bezzina, Elena Biagini, Nico A Blom, Rudolf A De Boer, et al. 2023 esc guidelines for the management of cardiomyopathies: developed by the task force on the management of cardiomyopathies of the european society of cardiology (esc). *European heart journal*, 44(37):3503–3626, 2023. 1
- [3] Shuai Bai, Keqin Chen, Xuejing Liu, Jialin Wang, Wenbin Ge, Sibo Song, Kai Dang, Peng Wang, Shijie Wang, Jun Tang, et al. Qwen2. 5-vl technical report. *arXiv preprint arXiv:2502.13923*, 2025. 5, 7
- [4] Biykem Bozkurt, Monica Colvin, Jennifer Cook, Leslie T Cooper, Anita Deswal, Gregg C Fonarow, Gary S Francis, Daniel Lenihan, Eldrin F Lewis, Dennis M McNamara, et al. Current diagnostic and treatment strategies for specific dilated cardiomyopathies: a scientific statement from the american heart association. *Circulation*, 134(23):e579–e646, 2016. 2
- [5] Junying Chen, Chi Gui, Ruyi Ouyang, Anningzhe Gao, Shunian Chen, Guiming Hardy Chen, Xidong Wang, Zhenyang Cai, Ke Ji, Xiang Wan, et al. Towards injecting medical visual knowledge into multimodal llms at scale. In *Proceedings of the 2024 conference on empirical methods in natural language processing*, pages 7346–7370, 2024. 7
- [6] Matthew Christensen, Milos Vukadinovic, Neal Yuan, and David Ouyang. Vision–language foundation model for echocardiogram interpretation. *Nature Medicine*, 30(5):1481–1488, 2024. 1
- [7] B Gow, T Pollard, N Greenbaum, B Moody, A Johnson, E Herbst, JW Waks, P Eslami, A Chaudhari, T Carbonati, et al. Mimic-iv-echo: Echocardiogram matched subset (version 0.1). *PhysioNet*, 2023. 6
- [8] Daya Guo, Dejian Yang, Haowei Zhang, Junxiao Song, Peiyi Wang, Qihao Zhu, Runxin Xu, Ruoyu Zhang, Shirong Ma, Xiao Bi, et al. Deepseek-r1 incentivizes reasoning in llms through reinforcement learning. *Nature*, 645(8081):633–638, 2025. 7
- [9] Paul A Heidenreich, Biykem Bozkurt, David Aguilar, Larry A Allen, Joni J Byun, Monica M Colvin, Anita Deswal, Mark H Drazner, Shannon M Dunlay, Linda R Evers, et al. 2022 aha/acc/hfsa guideline for the management of heart failure: a report of the american college of cardiology/american heart association joint committee on clinical practice guidelines. *Journal of the American College of Cardiology*, 79(17):e263–e421, 2022. 1
- [10] Gregory Holste, Evangelos K Oikonomou, Márton Tokodi, Attila Kovács, Zhangyang Wang, and Rohan Khera. Complete ai-enabled echocardiography interpretation with multitask deep learning. *JAMA*, 2025. 1, 2, 7, 3
- [11] Zhongzhen Huang, Linjie Mu, Yakun Zhu, Xiangyu Zhao, Shaoting Zhang, and Xiaofan Zhang. Elicit and enhance: Advancing multimodal reasoning in medical scenarios. *arXiv preprint arXiv:2505.23118*, 2025. 1, 2, 3
- [12] Michelle M Kittleson, Gurusher S Panjrathe, Kaushik Amacherla, Leslie L Davis, Anita Deswal, Dave L Dixon, James L Januzzi Jr, and Clyde W Yancy. 2023 acc expert consensus decision pathway on management of heart failure with preserved ejection fraction: a report of the american college of cardiology solution set oversight committee. *Journal of the American College of Cardiology*, 81(18):1835–1878, 2023. 1
- [13] Yuxiang Lai, Jike Zhong, Ming Li, Shitian Zhao, and Xiaofeng Yang. Med-r1: Reinforcement learning for generalizable medical reasoning in vision-language models. *arXiv preprint arXiv:2503.13939*, 2025. 1, 2, 3
- [14] Roberto M Lang, Michelle Bierig, Richard B Devereux, Frank A Flachskampf, Elyse Foster, Patricia A Pellikka, Michael H Picard, Mary J Roman, James Seward, Jack Shanewise, et al. Recommendations for chamber quantification. *European journal of echocardiography*, 7(2):79–108, 2006. 1
- [15] Roberto M Lang, Luigi P Badano, Victor Mor-Avi, Jonathan A Afifalo, Anderson Armstrong, Laura Ernande, Frank A Flachskampf, Elyse Foster, Steven A Goldstein, Tatiana Kuznetsova, et al. Recommendations for cardiac chamber quantification by echocardiography in adults: an update from the american society of echocardiography and the european association of cardiovascular imaging. *European Heart Journal-Cardiovascular Imaging*, 16(3):233–271, 2015. 1
- [16] Khai Le-Duc, Duy MH Nguyen, Phuong TH Trinh, Tien-Phat Nguyen, Nghiem T Diep, An Ngo, Tung Vu, Trinh Vuong, Anh-Tien Nguyen, Mau Nguyen, et al. S-chain: Structured visual chain-of-thought for medicine. *arXiv preprint arXiv:2510.22728*, 2025. 3
- [17] Yen-Ting Lin and Yun-Nung Chen. Llm-eval: Unified multi-dimensional automatic evaluation for open-domain conversations with large language models. *arXiv preprint arXiv:2305.13711*, 2023. 5
- [18] Mary S Minette and David J Sahn. Ventricular septal defects. *Circulation*, 114(20):2190–2197, 2006. 1
- [19] Carol Mitchell, Peter S Rahko, Lori A Blauwet, Barry Canaday, Joshua A Finstuen, Michael C Foster, Kenneth Horton, Kofo O Ogunyankin, Richard A Palma, and Eric J Velazquez. Guidelines for performing a comprehensive transthoracic echocardiographic examination in adults: recommendations from the american society of echocardiography. *Journal of the American Society of Echocardiography*, 32(1):1–64, 2019. 1
- [20] Jae K Oh, James B Seward, and A Jamil Tajik. *The echo manual*. Lippincott Williams & Wilkins, 2006. 1
- [21] Steve R Ommen, Carolyn Y Ho, Irfan M Asif, Seshadri Balaji, Michael A Burke, Sharlene M Day, Joseph A Dearani, Kelly C Epps, Lauren Evanovich, Victor A Ferrari, et al. 2024 aha/acc/amssm/hrs/paces/scmr guideline for the management of hypertrophic cardiomyopathy: a report of the american

heart association/american college of cardiology joint committee on clinical practice guidelines. *Journal of the American College of Cardiology*, 83(23):2324–2405, 2024. 1

[22] Jiazen Pan, Che Liu, Junde Wu, Fenglin Liu, Jiayuan Zhu, Hongwei Bran Li, Chen Chen, Cheng Ouyang, and Daniel Rueckert. Medvilm-r1: Incentivizing medical reasoning capability of vision-language models (vlms) via reinforcement learning. *arXiv preprint arXiv:2502.19634*, 2025. 1, 2, 3, 7

[23] Yi Qin, Dinusara Sasindu Gamage Nanayakkara, and Xiaomeng Li. Multi-Agent Collaboration for Integrating Echocardiography Expertise in Multi-Modal Large Language Models . In *MICCAI*. Springer Nature Switzerland, 2025. 4

[24] Pengcheng Qiu, Chaoyi Wu, Shuyu Liu, Yanjie Fan, Weike Zhao, Zhuoxia Chen, Hongfei Gu, Chuanjin Peng, Ya Zhang, Yanfeng Wang, et al. Quantifying the reasoning abilities of llms on clinical cases. *Nature Communications*, 16(1):1–14, 2025. 6, 7

[25] Alec Radford, Jong Wook Kim, Chris Hallacy, Aditya Ramesh, Gabriel Goh, Sandhini Agarwal, Girish Sastry, Amanda Askell, Pamela Mishkin, Jack Clark, et al. Learning transferable visual models from natural language supervision. In *International conference on machine learning*, pages 8748–8763. PMLR, 2021. 3

[26] Shaohao Rui, Kaitao Chen, Weijie Ma, and Xiaosong Wang. Improving medical reasoning with curriculum-aware reinforcement learning. *arXiv preprint arXiv:2505.19213*, 2025. 1, 5

[27] Sraavya Sambara, Sung Eun Kim, Xiaoman Zhang, Luyang Luo, Shreya Johri, Mohammed Baharoon, Du Hyun Ro, and Pranav Rajpurkar. 3dreasonknee: Advancing grounded reasoning in medical vision language models. *arXiv preprint arXiv:2510.20967*, 2025. 2, 3

[28] Andrew Sellergren, Sahar Kazemzadeh, Tiam Jaroensri, Atilla Kiraly, Madeleine Traverse, Timo Kohlberger, Shawn Xu, Fayaz Jamil, Cian Hughes, Charles Lau, et al. Medgemma technical report. *arXiv preprint arXiv:2507.05201*, 2025. 7

[29] Zhihong Shao, Peiyi Wang, Qihao Zhu, Runxin Xu, Junxiao Song, Xiao Bi, Haowei Zhang, Mingchuan Zhang, YK Li, Yang Wu, et al. Deepseekmath: Pushing the limits of mathematical reasoning in open language models. *arXiv preprint arXiv:2402.03300*, 2024. 5, 2

[30] Frank E Silvestry, Meryl S Cohen, Laurie B Armsby, Nitin J Burkule, Craig E Fleishman, Ziyad M Hijazi, Roberto M Lang, Jonathan J Rome, and Yan Wang. Guidelines for the echocardiographic assessment of atrial septal defect and patent foramen ovale: from the american society of echocardiography and society for cardiac angiography and interventions. *Journal of the American Society of Echocardiography*, 28(8):910–958, 2015. 1

[31] Per Anton Sirnes, Michal Tendera, Panos Vardas, and Petr Widimsky. Guidelines for the diagnosis and treatment of pulmonary hypertension. *European Heart Journal*, 30(20):2493–537, 2009. 1

[32] Shanshan Song, Yi Qin, Honglong Yang, Taoran Huang, Hongwen Fei, and Xiaomeng Li. Echoviewclip: Advancing video quality control through high-performance view recognition of echocardiography. In *MICCAI*, pages 181–191. Springer, 2025. 4

[33] Karen K Stout, Curt J Daniels, Jamil A Aboulhosn, Biykem Bozkurt, Craig S Broberg, Jack M Colman, Stephen R Crumb, Joseph A Dearani, Stephanie Fuller, Michelle Gurvitz, et al. 2018 aha/acc guideline for the management of adults with congenital heart disease: a report of the american college of cardiology/american heart association task force on clinical practice guidelines. *Journal of the American College of Cardiology*, 73(12):e81–e192, 2019. 1

[34] Yanzhou Su, Tianbin Li, Jiyao Liu, Chenglong Ma, Junzhi Ning, Cheng Tang, Sibo Ju, Jin Ye, Pengcheng Chen, Ming Hu, et al. Gmai-vl-r1: Harnessing reinforcement learning for multimodal medical reasoning. *arXiv preprint arXiv:2504.01886*, 2025. 1, 2, 3

[35] Haoran Sun, Yankai Jiang, Wenjie Lou, Yujie Zhang, Wenjie Li, Lilong Wang, Mianxin Liu, Lei Liu, and Xiaosong Wang. Enhancing step-by-step and verifiable medical reasoning in mllms. *arXiv preprint arXiv:2506.16962*, 2025. 1, 2, 3, 7

[36] Ryutaro Tanno, David GT Barrett, Andrew Sellergren, Sumedh Ghaisas, Sumanth Dathathri, Abigail See, Johannes Welbl, Charles Lau, Tao Tu, Shekoofeh Azizi, et al. Collaboration between clinicians and vision–language models in radiology report generation. *Nature Medicine*, 31(2):599–608, 2025. 3

[37] Rahul Thapa, Andrew Li, Qingyang Wu, Bryan He, Yuki Sahashi, Christina Binder, Angela Zhang, Ben Athiwaratkun, Shuaiwen Leon Song, David Ouyang, et al. How well can general vision-language models learn medicine by watching public educational videos? *arXiv preprint arXiv:2504.14391*, 2025. 3

[38] Milos Vukadinovic, I-Min Chiu, Xiu Tang, Neal Yuan, Tien-Yu Chen, Paul Cheng, Debiao Li, Susan Cheng, Bryan He, and David Ouyang. Comprehensive echocardiogram evaluation with view primed vision language ai. *Nature*, pages 1–3, 2025. 1, 5, 7, 3

[39] Lehan Wang, Yi Qin, Honglong Yang, and Xiaomeng Li. Proactive reasoning-with-retrieval framework for medical multimodal large language models. *arXiv preprint arXiv:2510.18303*, 2025. 1, 2, 3, 5, 6, 7

[40] Chen Wei, Michael Milligan, Miranda Lam, Paul A Heidenreich, and Alexander Sandhu. Variation in cost of echocardiography within and across united states hospitals. *Journal of the American Society of Echocardiography*, 36(6):569–577, 2023. 1

[41] Susan E Wiegers, Thomas Ryan, James A Arrighi, Samuel M Brown, Barry Canaday, Julie B Damp, Jose L Diaz-Gomez, Vincent M Figueiredo, Mario J Garcia, Linda D Gillam, et al. 2019 acc/aha/ase advanced training statement on echocardiography (revision of the 2003 acc/aha clinical competence statement on echocardiography) a report of the acc competency management committee. *Journal of the American College of Cardiology*, 74(3):377–402, 2019. 1

[42] Weiwen Xu, Hou Pong Chan, Long Li, Mahani Aljunied, Ruifeng Yuan, Jianyu Wang, Chenghao Xiao, Guizhen Chen, Chaoqun Liu, Zhaodonghui Li, et al. Lingshu: A generalist foundation model for unified multimodal medical understanding and reasoning. *arXiv preprint arXiv:2506.07044*, 2025. 2, 6, 7

[43] An Yang, Anfeng Li, Baosong Yang, Beichen Zhang, Binyuan Hui, Bo Zheng, Bowen Yu, Chang Gao, Chengan Huang, Chenxu Lv, et al. Qwen3 technical report. *arXiv preprint arXiv:2505.09388*, 2025. 5

[44] Jiewen Yang, Yiqun Lin, Bin Pu, Jiarong Guo, Xiaowei Xu, and Xiaomeng Li. Cardiacnet: Learning to reconstruct abnormalities for cardiac disease assessment from echocardiogram videos. In *Computer Vision – ECCV 2024*, 2025. 6

[45] Ling Yang, Zhaochen Yu, Tianjun Zhang, Shiyi Cao, Minkai Xu, Wentao Zhang, Joseph E Gonzalez, and Bin Cui. Buffer of thoughts: Thought-augmented reasoning with large language models. *Advances in Neural Information Processing Systems*, 37:113519–113544, 2024. 2, 3

[46] Ling Yang, Zhaochen Yu, Bin Cui, and Mengdi Wang. Reasonflux: Hierarchical llm reasoning via scaling thought templates. *arXiv preprint arXiv:2502.06772*, 2025. 2, 3

[47] Jaehoon Yun, Jiwoong Sohn, Jungwoo Park, Hyunjae Kim, Xiangru Tang, Yanjun Shao, Yonghoe Koo, Minhyeok Ko, Qingyu Chen, Mark Gerstein, et al. Med-prm: Medical reasoning models with stepwise, guideline-verified process rewards. *arXiv preprint arXiv:2506.11474*, 2025. 3

[48] Jingyi Zhang, Jiaxing Huang, Huanjin Yao, Shunyu Liu, Xikun Zhang, Shijian Lu, and Dacheng Tao. R1-vl: Learning to reason with multimodal large language models via step-wise group relative policy optimization. *arXiv preprint arXiv:2503.12937*, 2025. 3, 7

[49] Yanzhao Zhang, Mingxin Li, Dingkun Long, Xin Zhang, Huan Lin, Baosong Yang, Pengjun Xie, An Yang, Dayiheng Liu, Junyang Lin, et al. Qwen3 embedding: Advancing text embedding and reranking through foundation models. *arXiv preprint arXiv:2506.05176*, 2025. 8, 1

[50] Jiaru Zou, Ling Yang, Jingwen Gu, Jiahao Qiu, Ke Shen, Jingrui He, and Mengdi Wang. Reasonflux-prm: Trajectory-aware prms for long chain-of-thought reasoning in llms. *arXiv preprint arXiv:2506.18896*, 2025. 3

# Incentivizing Cardiologist-Like Reasoning in MLLMs for Interpretable Echocardiographic Diagnosis

## Supplementary Material

### A. Data Construction Details

To curate a multiview, multimodal echocardiography dataset for complex cardiac disease diagnosis, we first retrieved patient records from 2022 to 2025 that included 15 targeted types of complex cardiac diseases as well as patients without detectable abnormalities. Table 5 lists all complex cardiac disease categories included in our study. In total, we retrieved 2109 patients. Each patient record comprises a complete echocardiography record, quantitative cardiac measurement data, and a clinical echocardiography report. The complete echocardiography record contains transthoracic echocardiography (TTE) 2D imaging, Color Doppler, M-Mode, Continuous Wave (CW) Doppler, and Pulse Wave (PW) Doppler acquisitions from multiple standard cardiac views. On average, each patient has 54 echocardiography records. This comprehensive study design mirrors the information available to cardiologists in routine clinical practice and is sufficient to support reliable echocardiography based diagnosis. We ensured that there is no overlap between the patients in the training and testing sets. We followed prior work [10, 38] to further process the raw echocardiography videos. All echocardiography videos are standardized to a spatial resolution of  $224 \times 224$  with 16 frames. All static contents (e.g., M-Mode and CW/PW Doppler) are resized such that the shortest side is 224 while preserving the original aspect ratio.

### B. Cardiac Reasoning Template Construction

**Cardiac Reasoning Template Construction Details** We curated the Cardiac Reasoning Template (CRT) from authoritative echocardiography knowledge sources, including a standard textbook [20] and disease specific clinical guidelines for each selected condition [2, 9, 12, 14, 18, 19, 21, 30, 31, 33, 41]. The textbook provides fundamental echocardiography principles, whereas the guidelines describe up to date diagnostic techniques for the corresponding diseases. We used GPT-5 to organize the CRT entries into structured templates, as illustrated in Fig. 5. The constructed CRT contains 42 templates in total. Each template has on average 7 steps, which reflects the necessity of multi step reasoning for complete and rigorous diagnosis. On average, each template consists of 335 words and specifies detailed echocardiographic views and measurements, thereby encoding rich cardiology knowledge. After constructing the CRT, we employed Qwen3-Embedding [49] to retrieve templates by selecting the one with the highest embedding similarity

between the disease query and the template metadata.

Cardiac Reasoning Template Structure
{ "Template name": Disease name and content summary, "Knowledge Tag": Keywords, "Description": Short paragraph summary, "Application Scenario": ["List of abnormalities that can be seen from echocardiography"], "Views needed": ["Echo View 1", "Echo View 2", ...], "Measurement needed": ["Echo Measurement 1", "Echo Measurement 2", ...], "Reasoning Flow" (the step to diagnose the disease): [Step 1: xx view check xx xx , exclude xx xx', 'Step 2: xx', 'Step3: xx'] }

Figure 5. The template structure of Cardiac Reasoning Template.

**Examples of Cardiac Reasoning Template.** Figure 6 presents a complete example template from the CRT. The template provides detailed step by step instructions for the reasoning MLLM to execute diagnostic procedures, such as confirming abnormalities, comparing with normal reference values, and formulating intermediate findings. In this way, the MLLM is explicitly guided to follow the intended diagnostic workflow, while CardiacMind’s reward design incentivizes the MLLM to reason toward the correct conclusion based on these well defined steps.

### C. Procedural Quality Reward Implementation Detail

#### C.1. Question List Conversion Implementation

Procedural Quality Reward must verify whether CardiacMind’s reasoning steps correctly address the key diagnostic procedures specified in the reasoning template, which imposes stringent requirements on the verifier to understand the logic and context in both the template and the model response. To simplify the evaluation of such logic intensive content, while still leveraging the high level diagnostic information encoded in the template, we convert the stepwise verification target from the original descriptive text into a list of questions associated with the analysis of echocardiographic views and measurements. Specifically, for each step in the template, we use GPT-5 to perform this conversion. Figure 7 illustrates the conversion process and shows the resulting question list used for verification. After the conversion, for each individual patient, we select the questions whose required views are present in that patient’s study, based on the annotated view labels and the view requirements in the template metadata.

#### C.2. Verifier Implementation Detail

We used Qwen3-8B as the backbone verifier for PQIR and ran it in non thinking mode for efficiency. We instructed the

Table 5. Selected diseases and their corresponding sample counts in the training set and EchoComplex. SVC: Superior Vena Cava. ASD: Atrial Septal Defect. VSD: Ventricular Septal Defect. PAH: Pulmonary Hypertension. HFpEF: Heart Failure with preserved Ejection Fraction. Normal indicates that no abnormality is identified in the patient’s echocardiographic report.

Disease Name	Training Set	EchoComplex	Disease Name	Training Set	EchoComplex
Ischemic Cardiomyopathy	118	54	Outlet VSD	38	10
Hypertrophic Cardiomyopathy	102	59	Muscular VSD	23	5
Dilated Cardiomyopathy	116	57	Perimembranous VSD	54	10
Rheumatic Cardiomyopathy	20	10	Atrial Myxoma	35	5
Ostium Secundum ASD	112	50	Left Atrial Thrombus	34	5
SVC type Sinus Venosus ASD	15	10	Ventricular Aneurysm	62	20
PAH	192	89	Fabry	72	15
HFpEF	113	50	Normal	380	174

verifier to assess each answer along four dimensions: view and measurement involvement, conclusion involvement, factual accuracy, and answer based relevance, and to output scores only in the range from 0 to 1. The complete prompt used for verification is provided in Tab. 6.

Table 6. Prompt for the LLM-as-Judge Verifier used in Procedural Quality Reward.

#### Prompt for Procedural Quality Reward

You are given a list of authoritative questions and a response generated by an AI model. You are also given a echocardiographic view list available for the AI model to analysis. Your task is to evaluate the response based on its accuracy and answer-based relevance to the questions asked. Provide a score between 0 and 1, where 1 indicates a perfect response that based all the answer on the echocardiographic available, provided affirmative or negative conclusions and addressed the questions, and 0 indicates a answer that is: all based on the unavailable echocardiographic views (indicating hallucination), failed to specifically answer any of the specific questions posed, or vague, or completely irrelevant, or no affirmative or negative conclusion is provided. Return your score only. /no\_think

## D. Model Implementation Details

### D.1. Prompt Design

To guide the model to output an ordered step by step diagnostic reasoning path, we first design a prompt template, as shown in Tab. 7. The model is instructed to perform stepwise reasoning that adheres to the input templates and explicitly incorporates the required views and measurements.

### D.2. Training Procedure

**Reinforcement Training Target** We used Group Relative Policy Optimization (GRPO) [29] as the reinforcement learning strategy. Specifically, for each training data, we sample a group of rollouts  $\{r_i\}_{i=1}^G$  from the policy model  $\pi_{\theta_{\text{old}}}$  and acquire the reward  $\sigma_i$ . The advantage  $\hat{A}_{i,t}$  is estimated as the standard score of the group rewards. The optimization

Table 7. Prompt for CardiacMind.

#### System Prompt for CardiacMind.

You are an expert cardiologist. You are given a series of echocardiographic inputs and a disease query. Your task is to diagnose the disease. You are also given a guideline that help you diagnose the disease. In your reasoning steps, you should think carefully to address the demand and questions raised in each step of the guideline using the input echocardiographic content. DO NOT COPY THE GUIDELINE. You should diagnose step-by-step based on the given echocardiographic inputs. You should output your reasoning process in steps carefully and the final diagnosis. In each step of your reasoning output, include the video name (view name) and the measurement name from the input that you used as evidence, and use the word in the input. If your reasoning conclusion is supportive based on TTE, give “Yes” final answer. Base your decision only on current TTE input. The reasoning process and answer are enclosed within `<think> </think>` and `<answer> </answer>` tags, respectively, i.e., `<think> Step 1: xx; Step 2:xx </think><answer> answer here (Yes/No) </answer>`

target used for training is given as Eq. (5):

$$\mathcal{J}_{\text{GRPO}}(\theta) = \mathbb{E}_{x, \{r_i\}_{i=1}^G \sim \pi_{\theta_{\text{old}}}(\cdot | x, T)} \left\{ \frac{1}{G |r_i|} \sum_{i=1}^G \sum_{t=1}^{|r_i|} \min \left[ \rho_{i,t} \hat{A}_{i,t}, \text{clip}(\rho_{i,t}, 1 - \epsilon, 1 + \epsilon) \hat{A}_{i,t} \right] - \beta \mathbb{D}_{\text{KL}} \left[ \pi_{\theta}(\cdot | x, T) \parallel \pi_{\theta_{\text{ref}}}(\cdot | x, T) \right] \right\}. \quad (5)$$

Here,  $\beta$  is the KL divergence penalty coefficient that controls the degree of exploration by the policy model.

**Implementation Settings.** All experiments are conducted on 32 H800 GPUs using SWIFT as the training framework. For GRPO training, we perform full parameter fine tuning with a learning rate of  $2e^{-6}$  and  $\beta$  set to  $5e^{-3}$  in the first training stage and  $1e^{-2}$  in the second stage, and optimize the model using DeepSpeed with ZeRO-2.

## E. Evaluation Implementation Details

### E.1. Baseline Model Implementation

We provide implementation details for all baseline methods in Tab. 1. All MLLM baselines, except “Qwen2.5-VL-ICL”, are evaluated without inserting retrieved templates from CRT, in order to benchmark their original echocardiography analysis capability. We use the recommended generation configurations with thinking mode, following the official implementations for each baseline. Below we provide additional explanations for specific baselines for clarity.

**EchoPrime [38].** EchoPrime is a CLIP [25] based vision language model that predicts diseases through video text similarity matching. Since EchoPrime is trained using large scale single video text contrastive learning, we perform direct video text similarity matching at test time to preserve its visual language representations. We follow the original implementation and recommended practice to perform prediction on all test data. Specifically, we use the original repository to select the diagnostic phrase with the highest embedding cosine similarity as the disease prediction. We perform per disease binary classification to report performance. For example, we choose between the sentences “Findings consistent with pulmonary hypertension.” and “PA systolic pressure is normal.” and take the one with the higher video text similarity as the final prediction.

**PanEcho [10].** PanEcho is a transformer based multi task predictor for 23 heart diseases that relies on disease specific classification heads for diagnosis. However, the original implementation does not include classification heads for the complex cardiac diseases considered in this paper. Therefore, we use PanEcho’s pretrained weights and released fine tuning code and configurations as the backbone, and fine tune 15 new single layer binary classification heads. We then use the fine tuned model to perform prediction on the entire test set.

**R1-VL [48].** We follow the design of R1-VL [48] and use a keyword matching approach as the “StepRAR” reward function, where the keywords include view names and cardiac measurement terms. All other rewards in R1-VL remain unchanged. We apply this setting to fine tune the Qwen2.5-VL-7B model for a fair comparison.

**MedVLM-R1 [22].** MedVLM-R1 deploys basic rewards in GRPO to perform reinforcement learning, which overlaps with the setting used in the “Qwen2.5-VL-GRPO” row. We therefore perform direct inference without additional fine tuning for brevity.

**Chiron-o1 [22].** Chiron-o1 proposes an LLM based data construction method for reasoning path generation, followed by supervised fine tuning on the constructed data. However, Chiron-o1 assumes that the MLLM used for reasoning path construction already has strong reasoning ability on the target modality and has been exposed to rich data. This assumption does not hold in the echocardiography domain, where open

source MLLMs still need to be explicitly incentivized for accurate echocardiography analysis [37]. Consequently, it is difficult to apply Chiron-o1’s data construction method to our data. We therefore directly infer with the official Chiron-o1 checkpoint for testing.

**MedRwR [39].** MedRwR proposes a method to retrieve external information during reasoning. However, the training rewards in MedRwR require constructing a broad echocardiography video based knowledge database with multi video input, and there is currently no sufficient publicly available dataset to satisfy this requirement. Therefore, fully reproducing the MedRwR training setup falls outside the scope of this paper, and we directly use the released MedRwR implementation for testing.

### E.2. Reasoning Score

We apply an LLM-as-Judge strategy to evaluate the quality of the reasoning path. Specifically, we use GPT-5 to assess reasoning paths along five dimensions:

- **Factual Quality.** Are the statements and interpretations medically and factually correct?
- **Coherence and Structural Logic.** Does the reasoning follow a clear, deductive, stepwise logic to confirm the presence of disease, assess chamber and valve morphology, quantify findings, and rule out artifacts and alternative structures?
- **Relevance and Focus.** Does the reasoning stay on topic and directly support the given question and final answer?
- **Informative and Analytic Value.** To what extent does the reasoning process use evidence from the input to analyze and support intermediate conclusions, rather than directly stating these conclusions without justification?
- **Echo Rigor and Validation.** Does the reasoning process explicitly mention echocardiography views and measurements, base its analysis on them, and address uncertainty with appropriate caution, instead of relying on generic statements (for example, describing only “the image” or “the video” without echo specific details)?

The final overall score is given on a scale from zero to five. We ran the assessment on all reasoning paths generated for EchoComplex.

### E.3. Reasoning Path Clinical Validation

We further invited a cardiologist to conduct a double-blinded paired-preference user study, following a setting similar to that in [36], to assess reasoning quality from a cardiology perspective. We first randomly sampled 30 patients from 7 cardiac disease categories in EchoComplex, namely Dilated Cardiomyopathy, HFP EF, Hypertrophic Cardiomyopathy, Ischemic Cardiomyopathy, Ostium Secundum ASD, Rheumatic Cardiomyopathy, and Ventricular Aneurysm. For each selected patient, we used CardiacMind and LingShu-7B to generate both the reasoning path and the final diagnostic

conclusion. We then anonymized the model identities and randomly permuted the order of the paired responses so that the cardiologist was blinded to the source. The cardiologist was instructed to select the reasoning path with higher quality according to three criteria. **Cardiologist’s Logic** evaluates which option is more aligned with standard cardiology diagnostic reasoning. **Clear and Deductive** evaluates which option presents clearer, more deductive, stepwise logic that confirms the presence of relevant findings, assesses adherence and morphology, quantifies observations, and rules out artifacts or other structures. **View and Measurement Involvement** evaluates which option more precisely specifies echocardiographic views and measurements, grounds its analysis in these elements, and addresses uncertainty with appropriate caution, rather than relying on generic references (e.g., “the image” or “the video”). For each pair, the cardiologist could choose option A, option B, or a neutral preference.

## F. Template-guided Reasoning Rectification Implementation Detail

We further performed template-guided reasoning rectification to identify and correct reasoning responses with low procedural adherence to the template, thereby improving diagnostic accuracy. Low template procedural adherence suggests that the reasoning path may deviate from the anchor diagnostic procedure and is therefore more likely to overlook or misinterpret critical information.

To identify low-adherence responses, we first generated a reasoning path for each test case. We then reused the verifier and scoring criteria described in Procedural Quality Rewards to rate the quality of each individual step in every reasoning path. After obtaining the stepwise reasoning quality scores, we averaged them within each case to obtain a single reasoning quality score per test example. Cases whose average score fell below a predefined threshold were subjected to a second round of reasoning.

For these low-scoring cases, we first identified the low-quality reasoning steps by selecting those steps with scores lower than the case-wise average minus one median absolute deviation. We then prompted the model with the previous conclusion and the identified low-quality steps, asking it to reconsider its reasoning and update the conclusion if necessary. The revised conclusion was taken as the final output for that case.

## G. Case Studies

We provide detailed reasoning outputs of CardiacMind with case studies in this section. Section G.1 presents examples of CardiacMind’s reasoning on both diseased and normal patients. Section G.2 presents a reasoning example in which CardiacMind is augmented with Template-guided Reason-

ing Rectification. Section G.3 presents reasoning examples used in the ablation studies. Note that all multimodal inputs comprise a complete echocardiography record, and we only illustrate four echocardiographic views in the figures for brevity.

### G.1. Examples of CardiacMind’s Reasoning Path

Figure 8 demonstrates CardiacMind’s reasoning process for a patient with dilated cardiomyopathy. The reasoning explicitly confirms quantitative echocardiographic measurements within the reasoning steps, such as “LVEDVi (biplane indexed) = 10.8 cm/m<sup>2</sup>, LVESVi (biplane indexed) = 10.7 cm/m<sup>2</sup>”, and associates cardiac clinical manifestations with the corresponding measurement abnormalities, for example “Global systolic dysfunction is noted with impaired deformation (GLS -3.2%) and sphericity index (ED) > 1.5”. It also specifies the echocardiographic views to inform cardiologists of the anatomical source of each piece of information. In steps 3 and 7, the reasoning process follows guideline-based practice to rule out potential confounders and etiologies (“No ischemic pattern is identified” and “No pericardial effusion”). Finally, the reasoning synthesizes these findings into a coherent diagnostic summary. Overall, for diseased patients, the reasoning identifies key abnormalities and explicitly links them to guideline-consistent diagnostic steps that support the final diagnosis.

Figure 9 shows CardiacMind’s reasoning for a negative patient. Following the reasoning template, the model systematically confirms the absence of abnormalities in a logically structured manner and ultimately rules out the possibility of the queried disease.

### G.2. Examples of CardiacMind’s Reasoning Path with Template-guided Reasoning Rectification.

Figure 10 illustrates the reasoning quality improvement achieved by template-guided reasoning rectification. In the first round of reasoning, the model’s reasoning path contains ungrounded and vague statements that lead to incorrect intermediate conclusions, such as “shows normal range” and “appear normal” in step 2, without referencing any quantitative measurements. This, in turn, results in an incorrect diagnosis. After template-guided reasoning rectification, the model is explicitly informed of the previously low-quality reasoning steps and subsequently provides detailed quantitative measurements before drawing conclusions, as in steps 2, 3, and 4. The improved reasoning process ultimately leads to a revised conclusion and a correct diagnosis.

### G.3. Ablative Case Studies

**Ablative Examples for Reward Functions.** Figure 11 shows the reasoning results when the reward components are gradually incorporated into the training process. When only

the basic accuracy and format rewards are applied, the model produces condensed outputs without explicit logical reasoning or detailed specification of views and measurements. When the procedural quantity reward is added, the reasoning path becomes more structured and follows a clearer logical order. However, the content remains abbreviated and often lacks grounded information, such as the vague phrase “evidence of remodeling”. When the Procedural Quality Reward is applied, the stepwise reasoning becomes more detailed and includes explicit references to echocardiographic views. When all rewards are applied together, they act synergistically to encourage the model to provide detailed measurements and view annotations, accompanied by observations that support the analysis and final conclusion, as illustrated in steps 1–3. This example highlights the distinct role and advantages of each proposed reward component.

**Ablative Examples for the Design Choice of PQIR.** Figure 12 shows the reasoning results for different design choices of Procedural Quality Rewards. When the model is verified directly against an overall descriptive paragraph, the reward model cannot provide comprehensive feedback on how the reasoning output addresses the critical questions in the given templates, which leads to an abbreviated reasoning process with descriptions not directly addressing vital diagnostic questions. When PQIR uses a simple strategy that maximizes first-sentence similarity to promote contextual relevance, the reasoning model tends to replicate or rephrase the original template (see bold red text in Fig. 12) without further analysis or additional conclusions. This increases the verbosity of the model while reducing the informativeness of the reasoning process.

## Cardiac Reasoning Template Example

```
{  
  "Template name": "HFpEF — Resting TTE confirmation (E/e', PASP, LA/LV morphology)",  
  "Knowledge Tag": "HFpEF, diastolic dysfunction, E/e', PASP, LAVI, LV mass index, ACC ECDP, H2FPEF",  
  "Description": "Use resting transthoracic echocardiography to confirm preserved LVEF and demonstrate elevated LV filling pressures with supportive structural remodeling. Strong echo evidence includes E/e' ≥15 and/or estimated PASP >35 mmHg, with increased LA volume index and/or LV mass index supporting the diagnosis of HFpEF. If findings are indeterminate, diastolic stress echocardiography can be helpful in further evaluation. ",  
  "Application Scenario": [  
    "Dyspnea with preserved LVEF on echo and no significant valve disease/ischemia on TTE",  
    "Elevated filling pressures at rest: high E/e' or pulmonary hypertension on Doppler (PASP >35 mmHg)",  
    "Structural support: increased LA volume index and/or LV mass index",  
    "Borderline diastolic parameters where stress echo data may clarify elevated filling pressures"  
,  
  "Views needed": [  
    "A4C",  
    "A2C",  
    "PLAX left ventricle",  
    ...  
,  
  "Measurement needed": [  
    "LVEF (biplane)",  
    "MV E velocity",  
    ...  
,  
  "Reasoning Flow": [  
    "Step 1: Confirm preserved systolic function and screen for alternative causes. From <view>A4C</view> and <view>A2C</view>, verify that <measure>LVEF (biplane)</measure> is ≥50% (preserved EF). From <view>PLAX left ventricle</view>, <view>PSAX (level of MV)</view>, and <view>PLAX left ventricle-Color</view>, visually assess for significant valvular disease (eg, moderate-severe AS/MS/MR) that could account for symptoms; HFpEF assessment presumes no significant valve disease or overt ischemia on TTE. ",  
    "Step 2: Mitral inflow (functional diastolic assessment). From <view>A4C-MV-PW</view>, review <measure>MV E velocity</measure>, <measure>MV A velocity</measure>, <measure>E/A ratio</measure>, and <measure>MV deceleration time</measure> to characterize diastolic filling pattern and support interpretation of filling pressures in conjunction with tissue Doppler. ",  
    "Step 3: Tissue Doppler e' and E/e' (filling pressures). From <view>A4C-MV-TDI-PW</view>, confirm <measure>Septal e'</measure> and <measure>Lateral e'</measure>, and calculate <measure>Average E/e'</measure>. An <measure>Average E/e'</measure> ≥15 is direct echo evidence of elevated LV filling pressures compatible with HFpEF; values >9 contribute to H2FPEF scoring. <image>",  
    "Step 4: TR velocity and PASP (pulmonary pressures). Using <view>PSAX (level great vessels) focus on TV-Color</view> to identify the TR jet and <view>PSAX (level great vessels) focus on TV-CW</view> to measure <measure>TR Vmax</measure>, and using <view>Subcostal long axis IVC</view> or <view>Subcostal long axis IVC-MMode</view> to estimate <measure>RAP (from IVC)</measure>, calculate <measure>PASP</measure>. A <measure>PASP</measure> >35 mmHg on Doppler echo supports HFpEF and contributes to H2FPEF scoring. <video>",  
    "Step 5: Left atrial size and LV structure (morphological support). From <view>A4C</view> and <view>A2C</view>, confirm <measure>LAVI</measure>. From <view>PLAX left ventricle</view> and/or <view>PLAX left ventricle-MMode</view>, review <measure>LV mass index</measure> and <measure>Relative wall thickness</measure>. Increased LA volume index and/or LV mass index represent key structural alterations that support the diagnosis of HFpEF when filling pressures are elevated. ",  
    "Step 6: Global longitudinal strain (optional supportive systolic metric). From <view>A4C zoomed left ventricle</view>, <view>A2C zoomed left ventricle</view>, and <view>Apical long axis zoomed left ventricle</view>, check <measure>GLS</measure> if available. GLS can aid broader phenotyping in HFpEF algorithms but is not a stand-alone diagnostic criterion in this TTE-only workflow. ",  
    "Step 7: Synthesize a TTE-based conclusion. Conclude HFpEF on TTE when <measure>LVEF (biplane)</measure> is preserved AND there is clear echo evidence of elevated LV filling pressures at rest (eg, <measure>Average E/e'</measure> ≥15 and/or <measure>PASP</measure> >35 mmHg), with structural support from increased <measure>LAVI</measure> and/or <measure>LV mass index</measure>. If <measure>Average E/e'</measure> is 9–14 or <measure>PASP</measure> near threshold, structural abnormalities strengthen the likelihood, while recognition that diastolic stress echocardiography can help in uncertain cases. "  
  ]  
}
```

Figure 6. Example of a template in the Cardiac Reasoning Template suite. In “Views Needed” and “Measurement Needed” sections, we shorten the lists of views and measurements for brevity, since the corresponding view and measurement names are already sufficiently specified in the “Reasoning Flow” section.

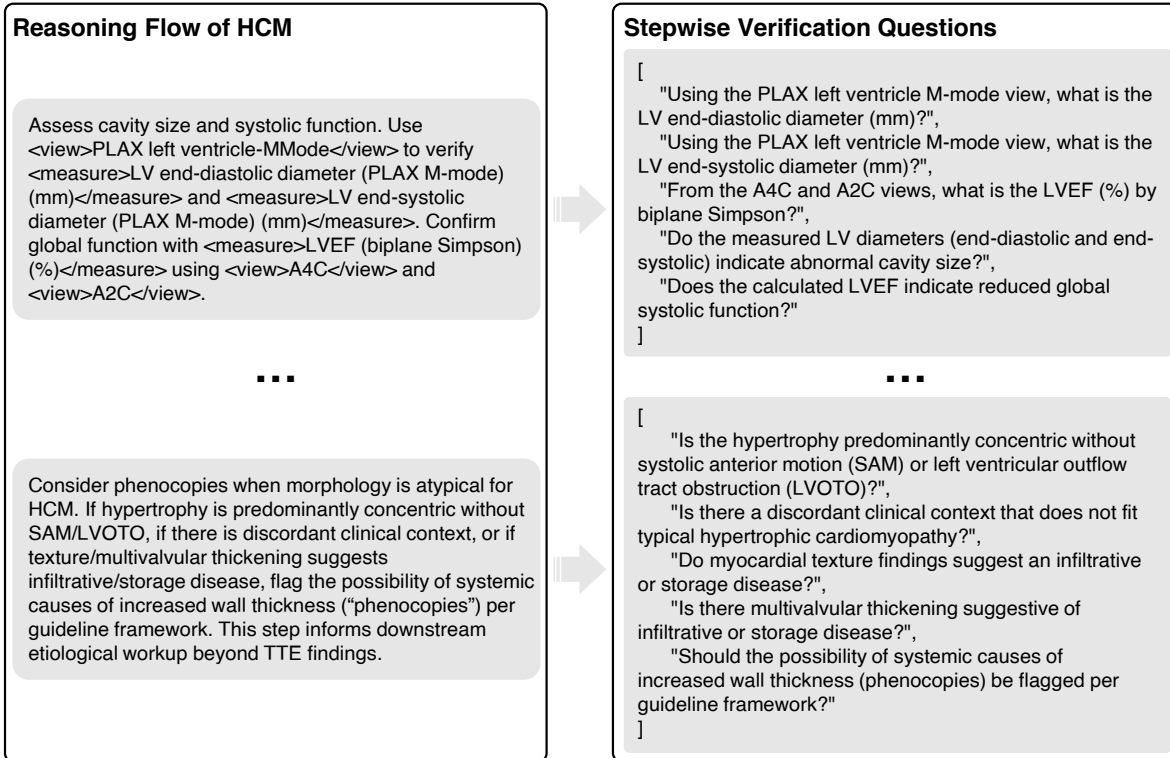
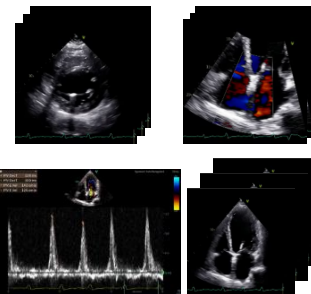


Figure 7. Example of converting steps in the reasoning flow of the Cardiac Reasoning Template into question lists. HCM: Hypertrophic Cardiomyopathy.

## Reasoning Example



"This is an echocardiography in A4C-Color: <video>. This is an echocardiography in A2C: <video>. ... Potential abnormalities pending to differentiate may include: Mild pulmonic regurgitation, Severely reduced left ventricular systolic function, .... Mild aortic valve calcification. <image> .... Potential abnormal measurements may include: Aortic-root cross-sectional area, Aortic-root diameter, Fractional shortening (M-mode), . The guideline that you should refer to: Step 1: Validate measurement integrity for volumetrics and EF. Review A4C and A2C used for Simpson biplane; confirm LVEDVi (biplane indexed), LVESVi (biplane indexed), and LVEF (biplane Simpson) were derived from the same recorded heartbeat to ensure internal consistency . .... Step 9: Final synthesis — Echo-based diagnosis of DCM. Conclude DCM when there is: (a) increased LV size (LVEDVi (biplane indexed) and/or LVEDD above normal), .... Please confirm whether the patient exhibits clinical manifestations of dilated cardiomyopathy? "

<think> Step 1: Measurement integrity for volumes and EF appears consistent. A4C and A2C used for Simpson biplane show LVEDVi (biplane indexed) = 10.8 cm/m<sup>2</sup>, LVESVi (biplane indexed) = 10.7 cm/m<sup>2</sup>, and LVEF (biplane Simpson) = 17%. All measurements appear internally consistent.

Step 2: LV dilation and global systolic dysfunction are evident. On A4C, A2C, Apical long axis (3C), and PLAX left ventricle, the LV is severely dilated with increased LVEDVi (biplane indexed) and reduced EF (17%). Global systolic dysfunction is noted with impaired deformation (GLS -3.2%) and sphericity index (ED) > 1.5. No regional wall motion abnormalities are observed.

Step 3: No regional or coronary territory wall motion abnormalities are observed in PSAX (level of papillary muscles), A4C, A2C, or Apical long axis (3C). No ischemic pattern is identified.

Step 4: No primary valve disease is identified. Regurgitation mechanisms in PLAX left ventricle-Color and A4C-Color suggest functional (secondary) MR (annular dilation, leaflet tethering). No primary leaflet pathology is observed. MR EROA, MR regurgitant volume, and vena contracta width are not severe.

Step 5: LV diastolic function is restrictive. E velocity (MV inflow) and A velocity (MV inflow) are elevated. E/A ratio is > 2. Mitral E-wave deceleration time is shortened. Septal and lateral e' velocities are reduced. Average E/e' is > 10. LA volume index is elevated. Restrictive filling is confirmed.

Step 6: RV size and function appear preserved. TAPSE and RV S' (TDI lateral annulus) are normal. RVOT/pulmonic Doppler in PSAX focus on PV and PA-RVOT-PW and PSAX focus on PV and PA-PA-PW do not reveal significant pulmonary hypertension. Estimated PASP is not elevated.

Step 7: No apical opacification or thrombus detected on A4C-MCE, A2C-MCE, or Apical long axis (3C)-MCE. No functional MR or TR severity on PLAX left ventricle-Color or A4C-Color. No pericardial effusion seen on Subcostal long axis IVC.

Step 8: No LVOT VTI or area data available. No mechanical dispersion or stroke volume index quantified. No low-flow phenotype identified.

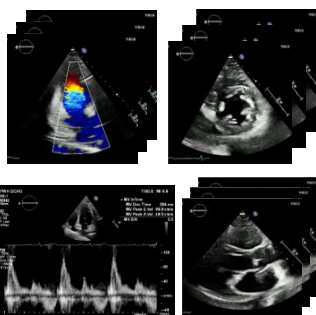
Step 9: Echocardiographic findings support DCM. Increased LV size (LVEDVi (biplane indexed) and LVEDD), reduced global systolic function (LVEF (biplane Simpson) and impaired GLS (3-plane)), global rather than regional wall motion abnormalities, and absence of primary valve cause of dilation. Supportive findings include elevated filling pressures, LA enlargement, RV involvement, and functional MR.

</think>

**<answer>Yes</answer>**

Figure 8. Example of CardiacMind's reasoning process for a diseased patient with dilated cardiomyopathy. Text in bold green indicates correct statements.

## Reasoning Example



This is an echocardiography in PLAX left ventricle: <video>. This is an echocardiography in PSAX focus on PV and PA-Color: <video> ... Potential abnormalities pending to differentiate may include: Mild tricuspid regurgitation, Mild mitral regurgitation... <image> .... Potential abnormal measurements may include: Interventricular-septal thickness in systole (2-D), ... The guideline that you should refer to:

Step 1: Confirm global LV systolic dysfunction and remodeling using A4C, A2C, and Apical long axis (3C); verify volumetric and EF measurements: LVEF (biplane Simpson), LVEDVi, LVESVi, and deformation: Global longitudinal strain (GLS, %). Cross-check chamber geometry and wall thickness on PLAX left ventricle and circumferential shape on PSAX (level of papillary muscles). A comprehensive baseline echo dataset is recommended for cardiomyopathy evaluation .

...

Does the patient present with ischemic cardiomyopathy?

<think> Step 1: No global LV systolic dysfunction or remodeling is observed on A4C, A2C, and Apical long axis (3C). Volumetric and EF measurements (biplane Simpson) are normal. Chamber geometry and wall thickness appear normal on PLAX left ventricle and PSAX (level of papillary muscles). No significant deformation abnormalities (GLS) are noted.

Step 2: No regional wall motion abnormalities (hypokinesis, akinesis, dyskinesis) are identified on A4C, A2C, Apical long axis (3C), PSAX (level of MV), PSAX (level of papillary muscles), and PSAX (level of apex). No WMSI or territory-based strain documented.

Step 3: No end-diastolic wall thinning ( $\approx 6$  mm), persistent akinesis/dyskinesis, or contour bulge in systole/diastole are observed on PLAX left ventricle, A4C, A2C, Apical long axis (3C), or apical short axis PSAX (level of apex). No scar surrogate or aneurysm detected.

Step 4: No secondary (ischemic) mitral regurgitation from leaflet tethering is identified on A4C-Color and PLAX left ventricle-Color. No quantifiable EROA or regurgitant volumes. No apical tethering noted. No restrictive MR with apical tethering.

Step 5: No significant TR peak velocity on PSAX (level great vessels) focus on TV-CW. No evidence of elevated pulmonary pressures. RV function appears preserved on A4C RV-focused with normal TAPSE values. No RV dysfunction noted.

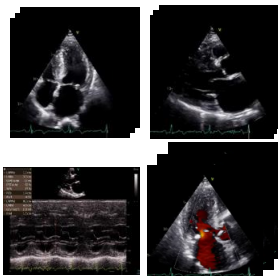
Step 6: No LV thrombus detected on A4C, A2C, Apical long axis (3C), or PSAX (level of apex).

</think>

**<answer>No</answer>**

Figure 9. Example of CardiacMind's reasoning process for a patient without ischemic cardiomyopathy. Text in bold green indicates correct statements.

## Reasoning with Template-guided Reasoning Rectification Example



This is an echocardiography in PLAX left ventricle: <video>. This is an echocardiography in PLAX RV inflow-Color: <video>. ... Potential abnormalities pending to differentiate may include: Mild to moderate mitral annular calcification, Trace mitral regurgitation.... The guideline that you should refer to:

Step 1: Confirm preserved systolic function and screen for alternative causes. From A4C and A2C, verify that LVEF (biplane) is  $\geq 50\%$  (preserved EF). From PLAX left ventricle, PSAX (level of MV), and PLAX left ventricle-Color, visually assess ... HFpEF assessment presumes no significant valve disease or overt ischemia on TTE.

Step 2: Mitral inflow (functional diastolic assessment). From A4C-MV-PW, review MV E velocity, MV A velocity, E/A ratio, and MV deceleration

...

Does this patient have HFpEF?

### Before Template-guided Reasoning Rectification

<think> Step 1: From A4C and A2C, LVEF (biplane) appears preserved at  $\geq 50\%$ . From PLAX left ventricle, PSAX (level of MV), and PLAX left ventricle-Color, no significant valvular regurgitations (AS/MS/MR) are observed.

Step 2: From A4C-MV-PW, **MV E velocity shows normal range, MV A velocity is elevated but not significantly so. Deceleration times appear normal.** No clear diastolic dysfunction.

Step 3: From A4C-MV TDI-PW, **septal e' and lateral e' are not clearly elevated. Average E/e' does not exceed 15.**

Step 4: No clear tricuspid regurgitation (TR) jet identified on PSAX (level great vessels) or Subcostal long axis IVC. **No clear PASP elevation suggested** on PSAX (level great vessels) or Subcostal long axis IVC.

Step 5: LAVI is mildly elevated on A4C and A2C. LV mass index is mildly elevated on PLAX left ventricle and PLAX left ventricle-Mode. No overt LV hypertrophy noted.

Step 6: No global longitudinal strain (GLS) data provided.

Step 7: LVEF preserved. No clear echo evidence of elevated LV filling pressures (Average E/e'  $\geq 15$  or PASP  $> 35$  mmHg). No clear structural support for elevated filling pressures.

Step 8: No clear Average E/e'  $> 9$  or PASP  $> 35$  mmHg on TTE.

</think>

<answer>No</answer>

### After Template-guided Reasoning Rectification

<think> Step 1: From A4C and A2C, LVEF (biplane) appears to be preserved,  $\geq 50\%$ . From PLAX left ventricle, PSAX (level of MV), and PLAX left ventricle-Color, there is no clear evidence of significant valvular disease (e.g., moderate-severe AS/MS/MR).

Step 2: **From A4C-MV-PW, MV E velocity is 12 m/s, MV A velocity is 8 m/s, E/A ratio is approximately 1.5, and MV deceleration time is normal.** Diastolic filling pattern does not suggest significant diastolic dysfunction.

Step 3: From A4C-MV TDI-PW, **septal e' is 15 cm/s, lateral e' is 17 cm/s. Average E/e' is  $\geq 15$ .**

Step 4: From PSAX (level great vessels) focus on TV-Color, mild tricuspid regurgitation (TR) is present with a jet. **TR Vmax measured on PSAX (level great vessels) focus on TV-CW is 30 cm/s. PASP estimated by Subcostal long axis IVC (CW Doppler) is around 35 mmHg.**

Step 5: LAVI (A4C and A2C) is increased. LV mass index and Relative wall thickness appear elevated (A4C and A2C).

Step 6: No GLS data available.

Step 7: LVEF (biplane) preserved. Clear evidence of elevated LV filling pressures (Average E/e'  $\geq 15$ , PASP  $> 35$  mmHg). Structural support includes increased LAVI and LV mass index.

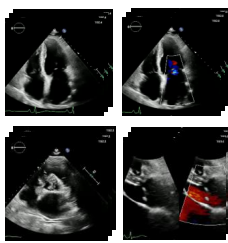
Step 8: Average E/e'  $> 9$  and PASP  $> 35$  mmHg.

</think>

<answer>Yes</answer>

Figure 10. Example of CardiacMind's reasoning process when augmented with template-guided reasoning rectification. Text in bold green indicates correct statements. Text in bold red indicates ungrounded and vague statements.

### Ablation on Reward Functions



This is an echocardiography in A4C-Color: <video>. This is an echocardiography in Apical long axis (3C): <video> ... Potential abnormalities pending to differentiate may include: Mildly reduced left ventricular systolic function ... <image> ... Potential abnormal measurements may include: LV ejection fraction - bi-plane Simpson... The guideline that you should refer to: Step 1: From A4C, identify any focal outpouching of the LV contour that persists in systole and diastole and exhibits dyskinesia (systolic expansion). Correlate global function with LVEF (Simpson or 3D), LVEDV (biplane), and LVESV (biplane) to document remodeling. These apical views are essential components of a complete TTE exam. Step 2: From A2C and Apical long axis (3C), confirm the outpouching in orthogonal planes to exclude foreshortening and pseudo-bulging, and measure geometry ...

...  
Based on the current information, does this patient have Ventricular Aneurysm?

### Format + Accuracy Reward

<think>Based on the provided echocardiography images and measurements, there is **no direct evidence of a ventricular aneurysm**. The images show **normal chamber sizes, normal wall thicknesses, and no focal wall motion abnormalities that would be expected in a ventricular aneurysm**. The apical akinesis noted could be due to other causes such as myocarditis, ischemia, or other cardiomyopathies, but it does not necessarily indicate a ventricular aneurysm.

Ventricular aneurysms typically present with focal wall thinning, abnormal wall motion, and often with a history of prior myocardial infarction. In this case, while there is some abnormal wall motion, the overall assessment of the images does not support the presence of a ventricular aneurysm.

It's important to note that a definitive diagnosis of a ventricular aneurysm requires a combination of clinical history, imaging findings, and sometimes additional tests like coronary angiography.</think>

<answer>no</answer>

### Format + Accuracy + Procedural Quantity Reward

<think> Step 1: The **A4C view shows a focal outpouching in the LV apex with dyskinesia**, which is consistent with an aneurysm. The EF is mildly reduced, and **there's evidence of remodeling**. Step 2: The A2C and Apical long axis views confirm the aneurysm, showing a broad neck and a thin-walled structure. Step 3: There's no obvious communication between the aneurysm and the LV cavity, suggesting a true aneurysm. Step 4: No obvious thrombus is seen. Step 5: The aneurysm has a broad neck and appears to be true. Step 6: There's significant regional dysfunction in the aneurysmal segment. Step 7: Moderate MR is present, and the LA is moderately dilated. Step 8: The aneurysm neck is broad compared to the aneurysm size.

</think>

<answer>Yes</answer>

### Format + Accuracy + Procedural Quantity + Procedural Quality Reward

<think> Step 1: From A4C, there is a focal outpouching at the apex that persists in systole and diastole with dyskinesia. **LVEF appears mildly reduced, and LVEDV and LVESV are elevated, suggesting remodeling**. Step 2: From A2C and Apical long axis (3C), the outpouching is confirmed in orthogonal planes. The aneurysm's maximal diameter in diastole and systole is measured, and no significant foreshortening is noted. No clear aneurysm length is identified. Step 3: On PSAX (apex) and PSAX (papillary muscles), the aneurysm shows circumferential extent with thinning of the wall. No clear scar or communication to the LV cavity is observed. No aneurysm neck diameter is measurable. Step 4: No thrombus is detected on A4C-MCE, A2C-MCE, or Apical long axis (3C)-MCE. Step 5: No persistent outward bulge with a broad neck is seen. No swirling or high-velocity jets are observed. Step 6: Global and regional mechanics reveal severe dyskinesia in the involved segment. Step 7: Moderate MR is present, with a diastolic profile consistent with MR. LA volume is moderately dilated. Step 8: Aneurysm neck diameter is not clearly defined compared to the aneurysm's maximal diameter.

</think>

<answer>Yes</answer>

### Format + Accuracy + Procedural Quantity + Procedural Quality + Echo Semantic Reward

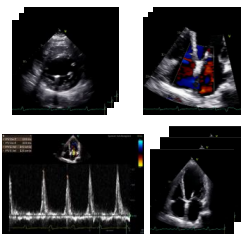
<think> Step 1: From A4C, there is a focal outpouching of the LV contour in systole and diastole. It exhibits dyskinesia (apical akinesis). **Global LV systolic function is mildly reduced (EF ~38-40%). LVEF (Simpson) is 39%. LVEDV (biplane) and LVESV (biplane) are normal**. Step 2: From A2C and Apical long axis (3C), the outpouching is confirmed in orthogonal planes. The aneurysm maximal diameter (diastole) measures approximately 1.5 cm. Aneurysm maximal diameter (systole) measures approximately 1.3 cm. Aneurysm length appears to be less than 1 cm. Parasternal long- and short-axis imaging complement these findings. Step 3: From PSAX (level of apex) and PSAX (level of papillary muscles), the aneurysm has a circumferential extent involving the apical region. The wall appears thinned and scarred. **No significant wall thickening is noted. Aneurysm neck diameter appears broad, measuring approximately 0.5 cm. No significant thinning or scar of the aneurysm wall is observed**. Step 4: No obvious filling defects or thrombus adherent to the aneurysm are detected on A4C-MCE, A2C-MCE, or Apical long axis (3C)-MCE. Endocardial borders appear well-defined. Step 5: From PLAX left ventricle and PLAX left ventricle-Color, the aneurysm has a broad neck composed of thinned myocardium. No high-velocity neck jet or sluggish swirling is seen. No evidence of a pseudo-bulging or false aneurysm. Step 6: From apical planes, the LV GLS and Regional longitudinal strain in the aneurysmal segment show severely reduced/positive strain (dyskinesia). Step 7: From A4C-Color, MR is present. Diastolic profile shows mild MR. LA volumes (A4C/A2C biplane) are moderately dilated. No significant tricuspid regurgitation is noted. Step 8: Aneurysm neck diameter (approximately 0.5 cm) is relatively broad compared to the aneurysm maximal diameter (diastole ~1.5 cm). This is consistent with a true aneurysm.

</think>

<answer>Yes</answer>

Figure 11. Ablation examples for reward functions. Text in bold green indicates correct statements. Text in bold red indicates incorrect statements. Text in bold yellow indicates brief statements that lack detail. Zoom in for best viewing.

### Ablation on the Design of Procedural Quality Reward



"This is an echocardiography in A4C-Color: <video>. This is an echocardiography in A2C: <video>. ... Potential abnormalities pending to differentiate may include: Mild pulmonic regurgitation, Severely reduced left ventricular systolic function, ..., Mild aortic valve calcification. <image> .... Potential abnormal measurements may include: Aortic-root cross-sectional area, Aortic-root diameter, Fractional shortening (M-mode), . The guideline that you should refer to: Step 1: Validate measurement integrity for volumetrics and EF. Review A4C and A2C used for Simpson biplane; confirm LVEDVi (biplane indexed), LVESVi (biplane indexed), and LVEF (biplane Simpson) were derived from the same recorded heartbeat to ensure internal consistency . ... Step 9: Final synthesis — Echo-based diagnosis of DCM. Conclude DCM when there is: (a) increased LV size (LVEDVi (biplane indexed) and/or LVEDD above normal), .... Please confirm whether the patient exhibits clinical manifestations of dilated cardiomyopathy? "

### Verifying using Converted Questions

<think> Step 1: Measurement integrity for volumes and EF appears consistent. A4C and A2C used for Simpson biplane show LVEDVi (biplane indexed) = 10.8 cm/m<sup>2</sup>, LVESVi (biplane indexed) = 10.7 cm/m<sup>2</sup>, and LVEF (biplane Simpson) = 17%. All measurements appear internally consistent.

Step 2: LV dilation and global systolic dysfunction are evident. On A4C, A2C, Apical long axis (3C), and PLAX left ventricle, **the LV is severely dilated with increased LVEDVi (biplane indexed) and reduced EF (17%). Global systolic dysfunction is noted with impaired deformation (GLS -3.2%) and sphericity index (ED) > 1.5. No regional wall motion abnormalities are observed.**

Step 3: No regional or coronary territory wall motion abnormalities are observed in PSAX (level of papillary muscles), A4C, A2C, or Apical long axis (3C). No ischemic pattern is identified.

...  
Step 9: Echocardiographic findings support DCM. Increased LV size (LVEDVi (biplane indexed) and LVEDD), reduced global systolic function (LVEF (biplane Simpson) and impaired GLS (3-plane)), global rather than regional wall motion abnormalities, and absence of primary valve cause of dilation. Supportive findings include elevated filling pressures, LA enlargement, RV involvement, and functional MR.

</think>

<answer>Yes</answer>

### Verifying using Descriptive Paragraph

<think> Step 1: Measurement integrity for volumes and EF was confirmed using A4C and A2C for Simpson biplane. LVEDVi (biplane indexed), LVESVi (biplane indexed), and LVEF (biplane Simpson) were derived from the same recorded heartbeat, ensuring internal consistency.

Step 2: LV dilation and global systolic dysfunction are evident on A4C, A2C, Apical long axis (3C), and PLAX left ventricle. **Increased LVEDVi (biplane indexed) and enlarged linear dimensions LVEDD, LVESD are observed with reduced LVEF (biplane Simpson) and impaired deformation GLS (less negative than normal).**

Step 3: No ischemic pattern was identified in the PSAX (level of papillary muscles), A4C, A2C, or Apical long axis (3C) views.

...  
Step 9: The patient exhibits increased LV size (LVEDVi and LVEDD), reduced global systolic function (LVEF and impaired GLS), global rather than regional wall motion abnormalities, and no primary valve cause of dilation. Supportive findings include elevated filling pressures, LA enlargement, and functional MR.

</think>

<answer>Yes</answer>

### Verifying by Maximizing First Sentence Similarity

<think> Step 1: **Validating measurement integrity for volumetrics and EF. Reviewing A4C and A2C used for Simpson biplane; confirming LVEDVi (biplane indexed), LVESVi (biplane indexed), and LVEF (biplane Simpson) were derived from the same recorded heartbeat to ensure internal consistency.**

The LVEDVi (biplane indexed) and LVESVi (biplane indexed) appear consistent between the A4C and A2C. The LVEF (biplane Simpson) is reduced.

Step 2: **Confirming LV dilation and global systolic dysfunction. On A4C, A2C, Apical long axis (3C), and PLAX left ventricle, assessing chamber size/remodeling and wall motion pattern. Increased LVEDVi (biplane indexed) and/or enlarged linear dimensions LVEDD, LVESD with reduced LVEF (biplane Simpson) and impaired deformation GLS (3-plane) (less negative than normal).**

The A4C, A2C, Apical long axis (3C), and PLAX left ventricle show severe LV dilation and global systolic dysfunction. The LVEDVi is elevated, and the LVEF is severely reduced. The GLS is severely abnormal.

Step 3: **Excluding an ischemic pattern. Inspecting wall motion across coronary territories in PSAX (level of papillary muscles), A4C, A2C, and Apical long axis (3C). DCM typically shows diffuse global hypokinesis; the presence of regional, coronary-territory wall motion abnormalities suggests an ischemic etiology rather than primary DCM.**

The wall motion appears globally hypokinetic without any regional wall motion abnormalities. There's no evidence of ischemia.

...

Step 9: Final synthesis — Echo-based diagnosis of DCM. Conclude DCM when there is: (a) increased LV size (LVEDVi (biplane indexed) and/or LVEDD above normal), (b) reduced global systolic function (LVEF (biplane Simpson) reduced and impaired GLS (3-plane)), (c) global rather than regional wall motion abnormalities, and (d) absence of a primary valve cause of dilation, with supportive findings such as elevated filling pressures, LA enlargement, RV involvement, and functional MR/TR.

</think>

<answer>Yes</answer>

Figure 12. Ablation examples for design choices of the Procedural Quality Reward. Text in bold green indicates correct statements. Text in bold red indicates statements repeated from the given template. Text in bold yellow indicates brief statements that lack detail. Zoom in for best viewing.